

**The Role of Translocator Protein in Prostate Cancer:
Implications as a Therapeutic Target for Advanced Disease**

by

Arlee E. Fafalios

B.S. Allegheny College 2005

Submitted to the Graduate Faculty of
The School of Medicine in partial fulfillment
of the requirements for the degree of
Doctor of Philosophy

University of Pittsburgh

2009

UNIVERSITY OF PITTSBURGH
SCHOOL OF MEDICINE

This dissertation was presented

by

Arlee E. Fafalios

It was defended on

August 7th, 2009

and approved by

Marie C. DeFrances, MD, PhD
Dissertation Committee Chair
Assistant Professor, Department of Pathology

Zhou Wang, PhD
Professor, Department of Urology

Jean J. Latimer, PhD
Assistant Professor, Department of Pathology

Daniel E. Johnson, PhD
Associate Professor, Department of Medicine

Beth R. Pflug, PhD
Dissertation Advisor
Associate Professor, Department of Urology

**THE ROLE OF TRANSLOCATOR PROTEIN IN PROSTATE CANCER:
IMPLICATIONS AS A THERAPEUTIC TARGET FOR ADVANCED DISEASE**

Arlee E. Fafalios, PhD

University of Pittsburgh, 2009

Background

Prostate cancer is the second leading cause of cancer related death in men. Current therapies for metastatic prostate cancer can only prolong progression, as most men eventually succumb to metastasis and then death. Therefore, there is continued urgency to identify novel therapeutic targets for advanced disease. Previous reports have identified an increase in Translocator Protein (TSPO) expression in numerous cancer models, including prostate. Functionally, TSPO has been implicated in the regulation of apoptosis and cell proliferation. Here, the role of TSPO in advanced prostate cancer is evaluated in an effort to establish the potential value of TSPO as a therapeutic target in advanced disease.

Methodology and Principle Findings

Immunohistochemical analysis using tissue microarrays was used to determine the expression profile of TSPO in human prostate cancer tissues. We observed that TSPO expression increases with disease progression, as prostate cancer metastases had the highest expression. To demonstrate the effect of TSPO ligands PK11195 and lorazepam in prostate cancer, we utilized cell proliferation assays, cell death ELISAs, and a prostate cancer mouse xenograft study. Our findings provide the first evidence of the anti-tumor effects of lorazepam acting on TSPO. To determine the effect of modulating TSPO expression, we performed overexpression and

knockdown studies. These studies provided further evidence that lorazepam is acting through TSPO, as overexpression of TSPO conferred increased susceptibility to lorazepam while TSPO knockdown decreased susceptibility. Lastly, we investigated the role of TSPO multimers in prostate cancer. We found that TSPO multimers can be induced by reactive oxygen species and may be formed through a di-tyrosine covalent bond.

Conclusions and Significance

TSPO expression increases with prostate cancer progression. The benzodiazepine lorazepam exerts its anti-cancer effects through its binding to TSPO. Collectively, these data suggest that TSPO is an excellent therapeutic target for advanced disease and that our preclinical results demonstrating that the already existing FDA-approved drug lorazepam has anti-tumor effects could be easily translated to the prostate cancer patient population. These studies could lead to a significant change in the management of prostate cancer by providing a treatment option with minimal toxicity for use in advanced disease and could ultimately prevent prostate cancer deaths.

TABLE OF CONTENTS

PREFACE	XII
1.0 INTRODUCTION	1
1.1 PROSTATE DEVELOPMENT AND FUNCTION.....	1
1.2 PROSTATE CANCER INCIDENCE AND RISK FACTORS.....	3
1.3 PROSTATE CANCER TREATMENT.....	6
1.4 TRANSLOCATOR PROTEIN.....	8
1.4.1 Translocator Protein Function.....	8
1.4.2 Translocator Protein Pharmacologic Profile.....	9
1.4.3 Translocator Protein Structure and Di-Tyrosine Bonds.....	10
1.4.4 Translocator Protein and Apoptosis.....	10
1.4.5 Translocator Protein and Cholesterol.....	12
1.4.6 Translocator Protein and Cancer.....	13
1.5 PURPOSE.....	14
1.6 MATERIALS AND METHODS.....	14
1.6.1 Cell Lines and Culture Conditions.....	14
1.6.2 Tissue Microarrays and Immunohistochemistry.....	15
1.6.3 Immunoblotting.....	16
1.6.4 MTT Cell Viability Assay.....	18

1.6.5 Cell Proliferation Assay.....	18
1.6.6 Cell Death ELISA.....	19
1.6.7 Flow Cytometry.....	19
1.6.8 Combination Therapy Studies.....	20
1.6.9 TSPO Antagonism In Vivo.....	20
1.6.10 Immunohistochemistry.....	21
1.6.11 Tumor Growth Modeling.....	22
1.6.12 Stable Transfections.....	22
1.6.13 Susceptibility to Lorazepam and Cell Proliferation.....	23
1.6.14 Colony Formation Assay.....	24
1.6.15 Wound Healing Assay.....	25
1.6.16 Soft Agar Colony Formation Assay.....	25
1.6.17 Matrigel Invasion Assay.....	25
1.6.18 Mouse and Human Tissue.....	26
1.6.19 Transient TSPO Knockdown.....	26
1.6.20 Breaking Di-Tyrosine Bonds.....	27
1.6.21 Forming Di-Tyrosine Bonds.....	27
1.6.22 Reactive Oxygen Species Scavenger Studies.....	28
1.6.23 Targeting a Tyrosine for Site-Directed Mutagenesis.....	28
1.6.24 TSPO Construct Generation and Transfection.....	29
1.6.25 Reactive Oxygen Species Inducer and Multimer Formation.....	29
2.0 TSPO AS A REGULATOR OF CELL PROLIFERATION AND APOPTOSIS IN PROSTATE CANCER.....	30

2.1 INTRODUCTION	30
2.2 RESULTS	32
2.2.1 TSPO expression is increased in human prostate cancer.....	32
2.2.2 TSPO antagonism has anti-proliferative and pro-apoptotic effects in vitro.....	35
2.2.3 TSPO antagonism modulates survival and cell cycle-related proteins.....	38
2.2.4 In vitro analysis of combination TSPO antagonism and Taxotere (docetaxel) treatment in prostate cancer cells.....	39
2.2.5 TSPO Antagonism has Anti-Proliferative and Pro-Apoptotic Effects In Vivo.....	40
2.3 CONCLUSIONS.....	43
3.0 THE EFFECTS OF MODULATING TSPO EXPRESSION IN PROSTATE CANCER.....	45
3.1 INTRODUCTION.....	45
3.2 RESULTS.....	46
3.2.1 TSPO overexpression in HEK293 human kidney cells.....	46
3.2.2 The effect of TSPO overexpression on susceptibility to lorazepam.....	46
3.2.3 The effect of TSPO overexpression on cell proliferation.....	47
3.2.4 TSPO knockdown in PPC-1 human prostate cancer cells.....	48
3.2.5 The effect of TSPO knockdown on cell proliferation.....	49
3.2.6 The effect of TSPO knockdown on cells susceptibility to lorazepam... 	49
3.2.7 The effect of TSPO knockdown on cell migration.....	51

3.2.8 The effect of TSPO knockdown on cell growth in suspension.....	52
3.2.9 The effect of TSPO knockdown on cell invasion.....	53
3.3 CONCLUSIONS.....	54
4.0 THE ROLE OF TSPO MULTIMERS IN PROSTATE CANCER.....	56
4.1 INTRODUCTION.....	56
4.2 RESULTS.....	57
4.2.1 TSPO multimers in TRAMP and human tissue.....	57
4.2.2 Transient knockdown of TSPO multimers.....	58
4.2.3 8M Urea does not break di-tyrosine bonds.....	59
4.2.4 Hydrogen peroxide induces TSPO multimer formation.....	60
4.2.5 Reactive oxygen species scavengers increase TSPO monomers.....	60
4.2.6 Y34F Mutagenesis does not abolish TSPO multimer formation.....	62
4.2.7 Glucose oxidase increases TSPO monomers in MLL SDM cells.....	64
4.3 CONCLUSIONS.....	65
5.0 DISCUSSION.....	68
BIBLIOGRAPHY.....	79

LIST OF TABLES

Table 1. TSPO immunostaining in human prostate tissue by Gleason, stage, and PSA failure..... 35

LIST OF FIGURES

Figure 1. The adult human prostate gland.....	2
Figure 2. Cell types of a human prostatic duct.....	3
Figure 3. Di-tyrosine bond.....	10
Figure 4. TSPO expression is increased in human prostate cancer tissues.....	33
Figure 5. TSPO expression is increased in human prostate cancer cell lines.....	33
Figure 6. TSPO antagonism decreases cell viability in prostate cancer cells in vitro.....	36
Figure 7. TSPO antagonism decreases cell proliferation in prostate cancer cells in vitro... 	36
Figure 8. TSPO antagonism increases apoptosis in prostate cancer cells in vitro.....	37
Figure 9. Time course decrease of pAkt and induction of p27 expression by TSPO antagonism.....	38
Figure 10. Effect of combination docetaxel + PK11195/lorazepam on prostate cancer cell growth.....	40
Figure 11. TSPO antagonism decreases average prostate cancer tumor volume over time.....	42
Figure 12. TSPO antagonism decreases cell proliferation and increases apoptosis in prostate cancer cells in vivo.....	43
Figure 13. TSPO overexpression in HEK293 cells and TSPO antibody specificity.....	46

Figure 14. TSPO overexpression increases susceptibility to lorazepam in HEK293 cells...	47
Figure 15. TSPO overexpression has no effect on HEK293 cell proliferation.....	48
Figure 16. TSPO knockdown in PPC-1 cells.....	48
Figure 17. TSPO knockdown has differential effects on proliferation in PPC-1 shTSPO clones.....	49
Figure 18. TSPO knockdown has no effect on PPC-1 cells susceptibility to lorazepam by direct cell counting.....	50
Figure 19. TSPO knockdown decreases PPC-1 cells susceptibility by colony formation assay.....	51
Figure 20. TSPO knockdown decreases cell migration in PPC-1 cells.....	52
Figure 21. TSPO knockdown decreases PPC-1 cells ability to form colonies in suspension.....	53
Figure 22. TSPO knockdown decreases cell invasion in PPC-1 cells.....	54
Figure 23. TSPO multimers in TRAMP and human tissues.....	58
Figure 24. TSPO multimer status following transfection with TSPO siRNA.....	59
Figure 25. 8M Urea does not break TSPO multimer bonds.....	59
Figure 26. Hydrogen peroxide induces TSPO multimer formation in HEK293 cells.....	60
Figure 27. ROS scavengers increase TSPO monomers in MLL TSPO cells.....	61-62
Figure 28. TSPO structure and location of tyrosines.....	63
Figure 29. Site-directed mutagenesis of Y34 does not abolish TSPO multimer formation.....	64
Figure 30. Glucose oxidase increases the 18-kDa TSPO monomer in MLL TSPO SDM cells.....	65

PREFACE

In recognition of their scientific and intellectual contributions to this research, special thanks goes out to: Dr. Anil Parwani for his expertise in grading the tissue microarray data, Marie Aquafondata for her expert technical assistance in performing much of the immunohistochemistry, Dr. Moira Hitchens for her critical reading of manuscripts, and Dr. Robert Bies for his expertise in mathematical modeling of the *in vivo* mouse model data.

Enormous thanks to my dissertation advisor, Dr. Beth R. Pflug, for years of guidance and for helping me realize my potential as an independent scientist, as well as to my thesis committee for their assistance in the development of this research.

My biggest thanks goes to my mom, Linda, for her lifelong support, encouragement, and for being an example of how to prevail in spite of any obstacle. I want to thank my fiancé Austin, for being my personal scientific expert and my most passionate supporter, my best friends Vicki and Renee for always believing in me, my sister Nicole for pretending to understand science when I talked about my day, and my Gram for reminding me that everything always works out. Finally, I dedicate this work to my Grandpa Johnny, who beamed with pride when I brought home a 100% on spelling tests in elementary school, I can't even begin to imagine how proud he would be today.

1.0 INTRODUCTION

1.1 Prostate Development and Function

In 1543, Andreas Vesalius was the first to identify a small organ that he referred to in his anatomical drawings as a “male accessory sex gland” [1]. A century later a pioneer of human anatomy, Gerard Blasius, published a treatise on comparative anatomy that described what would later be termed the prostate, as “glandulae” surrounding the neck of the bladder [2]. In 1912, Lowsley reconstructed a newborn male prostate out of wax and this model provided a basis for illustrating the human prostate [3]. Several alternative models of prostate anatomy emerged over a period of 50 years and the currently accepted concept of prostate zones was eventually established in the early 1980s by a pathologist named John McNeal [4].

The beginning of human prostate growth begins around the 10th week of gestation and is induced by the production of testosterone by the fetal testis around 8 weeks. The initial outgrowths of the prostatic buds from the urogenital sinus (UGS) occur in response to the binding of 5 α -dihydrotestosterone (DHT) to androgen receptors localized in the surrounding mesenchymal tissue [5-7]. During the postnatal period, under the influence of androgens, the ducts form a lumen and the epithelium differentiates and begins synthesis of a variety of secretory products. Consistent among all the anatomical research on the prostate is the finding that origins of the prostatic ducts emerge in a ventral, lateral, and dorsal pattern from the UGS.

The zones described by McNeal differ from the lobes such that they are divided according to their function. The three zones include the central, peripheral, and transitional with the peripheral zone constituting up to 70% of prostate adenocarcinoma (figure 1). These lobes and zones are now the standard reference for understanding the normal and diseased prostate [8].

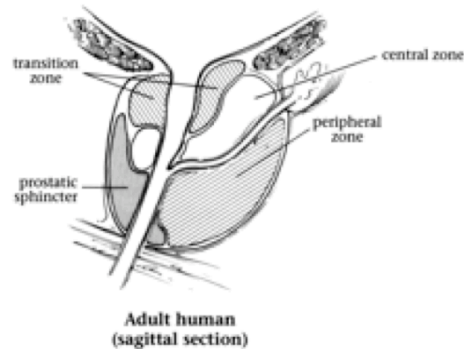


Figure 1. The adult human prostate gland.

Sagittal section of the adult human prostate gland showing the different zones of the prostate. (Adapted from Abate-Shen 2000)

Within the prostatic epithelium, there are three distinct cell types (figure 2). The predominant cell type is the secretory luminal cell, a differentiated androgen-dependent cell that produces prostatic secretory proteins. These cells are also characterized by their expression of androgen receptor. The second major epithelial cell type are the basal cells, which are found between the luminal cells and the underlying basement membrane, and which form a continuous layer in the human prostate. The third epithelial cell type found in the prostate gland is the neuroendocrine cell, a minor population of cells believed to provide paracrine signals that support the growth of the luminal epithelial cells. The luminal epithelial cells are the primary cell type to give rise to prostate carcinogenesis [9].

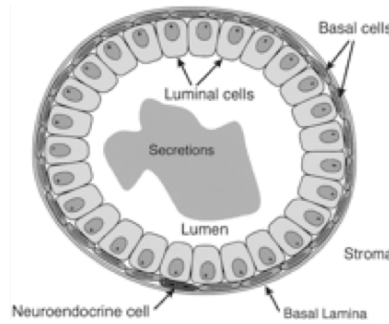


Figure 2. Cell types of a human prostatic duct.

(Adapted from Abate-Shen 2000)

As part of the male reproductive system, the prostate gland's primary role is to secrete a slightly alkaline fluid that constitutes approximately 25-30% of the volume of the seminal fluid. During ejaculation, the muscular glands of the prostate contract, propelling the fluid into the urethra where it combines with the sperm from the testes. The primary function of the prostatic fluid is to help neutralize the acidity of the vaginal tract, prolonging the lifespan of the sperm [10].

1.2 Prostate Cancer Incidence and Risk Factors

Prostate cancer is the most commonly diagnosed cancer in men, accounting for approximately 25% of new cancer diagnoses each year. Despite the continual decrease in prostate cancer mortality, it is estimated that nearly 29,000 men will die each year of prostate cancer-related deaths [11]. No definitive causes of prostate cancer have been identified; however, increasing age, a family history of the disease, and African American ancestry are strongly linked to its development [12].

Like many other cancers, incidence increases with age with more than 65% of all prostate cancers being diagnosed in men over the age of 65. Age is not the only risk factor however, as incidence and death rates vary considerably among racial and ethnic groups [11]. African American men are the most at risk population for developing prostate cancer and have a more than twofold greater chance of dying from the disease when compared to Caucasian men of European descent [11]. A review of prostate cancer mortality rates around the world showed that Western Europe, Australia, and North America had the highest rates, whereas the Far East and India had the lowest [12].

Differences in prostate cancer risk by race can be either endogenous, such as genetic differences or exogenous, such as dietary or detection. It is estimated that 9% of prostate cancer cases are due to an inherited predisposition [12]. For many years researchers struggled to find a genetic link to prostate cancer. It wasn't until fairly recently, through the development of gene expression arrays, that researchers discovered somatic mutations in prostate tumors. The most common mutation in prostate cancer is a gene fusion between the transmembrane protease serine 2 (TMPRSS2: 21q22.3) and a member of the erythroblast-transformation specific [13] gene family (ERG: 21q22.3) [14]. This fusion protein has been observed in approximately 50% of the tumors studied. TMPRSS2 is an androgen-regulated gene and ERG is a transcriptional regulator [15, 16]. Several *in vitro* studies have suggested that overexpression of ERG can result in invasive prostate cancer cells [17]. Fusion of these genes results in an androgen-dependent induction of oncogenic transcription factor overexpression. A study by Freedman *et al.* in 2006 identified that chromosome 8q24 is significantly associated with susceptibility to prostate cancer in African American men [18]. Furthermore, men carrying the BRCA gene are also at an increased risk for prostate cancer, among other cancers [19]. Although these few genetic

abnormalities have been identified, there is a continued effort to identify other genetic alterations using novel approaches such as genome-wide association studies which can detect germline single nucleotide polymorphisms (SNPs) associated with the disease [14].

A variety of dietary factors have been implicated in the development of prostate cancer according to epidemiologic studies of migrants, geographic variations, and temporal studies. Evidence has been presented that consistently demonstrates an association between dietary fat and prostate cancer, particularly the consumption of saturated fat and red meat [20-22]. Although an exact mechanism of action is unknown, the role of fat in increased prostate cancer incidence and mortality may be resulting from fat-induced alterations in hormonal profiles, the effect of fat metabolites as protein or DNA-reactive intermediates, or fat-induced elevation of oxidative stress [23].

Another possible explanation for the disparity in mortality between racial groups may lie in differences in detection and treatment. A recent study showed that African American men were significantly more likely than men of European descent to receive watchful waiting, which is an appropriate strategy for men with early-stage disease. This difference in undergoing watchful waiting was not fully explained by clinical characteristics or life expectancy at time of diagnosis, suggesting that other factors may be involved in this decision. These factors may include differences in access to health care resources, the patient desire to avoid treatment side effects or have the cancer removed, religious beliefs, and differences in the recommendations or preferences of physicians [24].

1.3 Prostate Cancer Treatment

Prostate specific antigen (PSA) is a serum protease that is expressed by epithelial prostate cells. It can be detected in the serum at low levels in men of all ages, but increases when the prostate enlarges. PSA is used as a biomarker for prostate cancer because as the prostate cancer cells grow, the normal organized structure of the prostate becomes disrupted which results in a release of PSA into the bloodstream [25]. Serum testing for prostate specific antigen (PSA) and a digital rectal examination (DRE) are the two initial procedures used to detect prostate cancer [26]. Elevated PSA levels and/or an abnormal DRE suggest the presence of prostate cancer, indicating the need for needle biopsies.

If diagnosed with localized, prostate-confined disease, a radical prostatectomy can be curative. However, for those patients whose cancer has penetrated the prostate capsule, disease recurrence is likely [27]. Regrowth of the tumor following initial treatment is usually androgen-dependent, relying on testosterone for survival and growth [28]. It is because of this dependency that androgen-ablation therapy, which induces apoptosis of androgen-dependent carcinoma cells, is the most common treatment for advanced prostate cancer. Unfortunately, through a combination of mechanisms that remain unclear, the vast majority of men will inevitably relapse with hormone-refractory prostate cancer (HRPC) [28]. HRPC is the lethal form of prostate cancer that progresses and metastasizes to distant organs. Chemotherapy has had very limited success in treating advanced prostate cancer therefore other therapeutic strategies must be employed.

The importance of androgens in the prostate was first identified over 50 years ago by Charles Huggins who observed prostate cancer regression upon removal of the testes [29]. Since

then, androgen ablation therapy has been the main therapy for advanced disease. Although removal of the testes is a very effective way to deplete androgen production, pharmacologic methods are much more preferred for blocking androgen function. Some of these agents include gonadotropin-releasing hormone (GnRH) super-agonists, androgen receptor antagonists, and 5 α -reductase inhibitors. GnRH agonists downregulate the GnRH receptor in pituitary gonadotropes, leading to the suppression of LH release and inhibition of testosterone secretion from the testis [28]. Androgen receptor antagonists, also called anti-androgens, bind with high affinity to the receptor thus blocking the binding of circulating testosterone or dihydrotestosterone (DHT) [28]. Finasteride is used to decrease the levels of cellular DHT, the active metabolite of testosterone, by blocking the activity of 5 α -reductase, the enzyme responsible for the conversion of testosterone to DHT [30].

Radiation is another therapeutic option for prostate cancer patients. Radiation therapy uses high-energy X-rays or gamma rays to kill the cancer cells. There are two ways in which the high-energy rays can be delivered. In external beam radiation therapy, a machine delivers the rays and the radiation is given in brief sessions. The procedure itself is painless and lasts for just a few minutes. The disadvantage to this treatment is that there is virtually no way to target only the cancer cells and as a result, both cancerous and some normal cells are exposed to the radiation. The other type of radiation used to treat prostate cancer is brachytherapy. In brachytherapy, the radiation comes from tiny, radioactive “seeds” inserted directly into the prostate. Brachytherapy allows the physician to use a higher dose of radiation than is possible with external beam radiation. Once the seeds are implanted they can continually give off rays for up to a year. Disadvantages of this treatment are the side effects that include impotence, urinary incontinence, and bowel problems.

Although these therapies are initially very effective, their efficacy decreases as the cancer progresses and metastasizes. The dynamics of the transition from androgen dependence to a state of independence are not fully understood, nor have all of the key molecular players been identified. Therefore, there is continued urgency in the scientific community to identify and study novel molecular targets involved in the complicated process leading to advanced disease.

1.4 Translocator Protein

1.4.1 Translocator Protein Function

Translocator protein (TSPO), previously known as the peripheral benzodiazepine receptor, was identified in 1977 [31]. The TSPO gene (*Bzrp*) is located on chromosome 22 (22q13.31) and is highly conserved throughout evolution [32]. The TSPO promoter in both rat and humans does not contain a TATA box, but does contain multiple Sp1 boxes [33], characteristic of a housekeeping gene. Knockout studies demonstrated that functional inactivation of the *Bzrp* gene induces an early embryonic-lethal phenotype [34]. TSPO is primarily localized to the mitochondria where it is best recognized for regulation of cholesterol transport from the outer to the inner mitochondrial membrane, the rate-determining step in steroidogenesis [35]. Although TSPO is widely expressed throughout the body, it is particularly enriched in steroidogenic tissues, such as gonads, adrenal gland, placenta and brain [36].

TSPO associates with peripheral benzodiazepine receptor (PBR)-associated protein 1, which interacts with the C-terminal end of TSPO and induces its dimerization [37], and protein

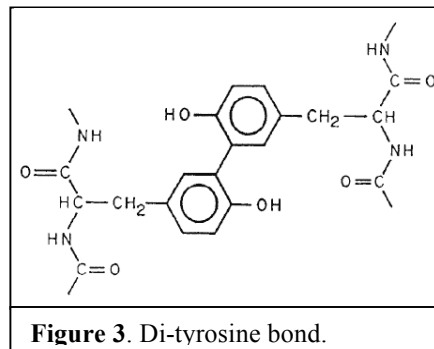
kinase A regulatory subunit RI α -associated protein, believed to recruit PKA to organelles rich in TSPO [38]. The 18-kDa TSPO also forms a multimeric complex with the adenine nucleotide translocase (ANT) and the voltage-dependent anion channel (VDAC), which is crucial for benzodiazepine binding [39]. Together these TSPO-associated proteins indicate two clearly identified functions of the TSPO: regulation of steroidogenesis and apoptosis [40].

1.4.2 Translocator Protein Pharmacologic Profile

As its earlier name suggests, the peripheral benzodiazepine receptor, now TSPO, binds benzodiazepines such as diazepam, 4-chlorodiazepam, lorazepam, or Ro5-4864 with relatively high (μ M) affinity [40]. Benzodiazepine receptors are found in both the central and peripheral nervous system, but unlike its central-type counterpart, TSPO has no anxiolytic or anticonvulsant effects and has distinct mechanistic and pharmacologic properties [41, 42]. There are also a wide variety of endogenous ligands that have been identified for TSPO including diazepam binding inhibitor (DBI; also called endozepine), porphyrins (protoporphyrins IX, heme) and cholesterol which bind with very high (nM) affinity. Binding studies have shown that lorazepam can inhibit binding of the high affinity TSPO ligand Ro5-4864 [43]. Although lorazepam is classically considered a ligand of the central-benzodiazepine receptor, the study by Park *et al.* suggests that it can also bind TSPO. The effects of lorazepam in peripheral tissue, such as the prostate, have yet to be explored.

1.4.3 Translocator Protein Structure and Di-Tyrosine Bonds

Structurally, TSPO is 18-kDa in size and consists of 5 transmembrane domains [44]. TSPO is primarily localized to the mitochondria where its 5 α -helices are embedded in the outer membrane [45]. TSPO antibodies have identified immunoreactive proteins of higher molecular weight than the



expected 18-kDa in cell and tissue extracts. A previous study reported that these higher molecular weight bands are the result of di-tyrosine bonds that covalently link TSPO monomers through reactions mediated by reactive oxygen species [46]. This linkage can occur between two tyrosine residues in the same molecule (intramolecular), or between two molecules (intermolecular); the latter leads to a higher molecular weight product [13]. Figure 3 shows di-tyrosine bond formed between two tyrosine residues.

1.4.4 Translocator Protein and Apoptosis

The mitochondrial permeability transition pore (MPTP) is a multiprotein complex that forms at the contact site between the inner and outer mitochondrial membranes and plays a critical role in apoptosis. The proteins VDAC, ANT, and TSPO are believed to make up this complex along with hexokinase, creatine kinase, and cyclophilin D; however, the exact protein composition of the MPTP continues to be debated [47]. Under normal physiological conditions the pore is dynamic, opening and closing to transport metabolites across the mitochondrial membrane in order to maintain transmembrane potential. The MPTP during apoptosis, however, is continuously open, releasing apoptotic factors into the cytosol, such as cytochrome c, Smac,

and apoptosis inducing factor [47]. The anti-apoptotic protein Bcl-2 interacts directly with VDAC and ANT and functions to suppress permeabilization of the mitochondrial membrane via the MPTP [48]. Without the inhibition of permeabilization by Bcl-2, the MPTP opens, liberating a flood of caspase and nuclease activators into the cytosol [47]. In this cascade of events, opening of the MPTP appears to be an irreversible step that commits the cell to undergo death, suggesting that opening of the MPTP is a point-of-no-return for apoptotic induction [49].

The opening of the MPTP, a critical step in the apoptotic process, leads to the disruption of the mitochondrial membrane integrity. The TSPO antagonist 1-(2-chlorophenyl)-*N*-methyl-*N*-(1-methylpropyl)-3-isoquinolinecarboxamide (PK11195) associates with the MPTP complex via its high-affinity binding to TSPO and promotes opening of the pore [50]. In cancer, failure of apoptotic induction leads to cellular resistance to anticancer therapies. Studies demonstrated that PK11195 enhances the sensitivity of cancer cells to tumor necrosis factor- α , CD95, and chemotherapeutic agents such as paclitaxel, docetaxel, and doxorubicin [51, 52]. Furthermore, numerous studies show that specific TSPO ligands can directly induce apoptosis in human cancer cells, including cells derived from hepatocellular, colorectal, and esophageal cancer [52-54]. Overexpression of the antiapoptotic regulator Bcl-2 confers cellular protection against chemotherapeutic agents, and this cytoprotective effect is largely reversed by PK11195 [50]. More recently, Li *et al.* reported that PK11195 disrupts mitochondrial integrity, directly resulting in release of cytochrome c into the cytosol [55]. Together these data supports that TSPO is intricately involved in the apoptotic process and that antagonism of TSPO may directly induce apoptosis in cancer cells.

1.4.5 Translocator Protein and Cholesterol

Aberrant cell proliferation and increased invasive and metastatic behavior are hallmarks of advanced prostate cancer. Previous studies propose a role for cholesterol in the mechanisms underlying cell proliferation and prostate cancer progression. Prostate cancer cells process critical cell survival cues via specialized membrane microdomains that are dependent on cholesterol for signal transduction [56]. TSPO is a high-affinity cholesterol-binding protein with its primary known role to transport cholesterol across the mitochondrial membrane [34, 35]. Although the primary function of TSPO is the regulation of steroidogenesis in the mitochondria, TSPO expression in nonsteroidogenic tissues as well as in other cellular compartments, including the nucleus, suggests that there may be alternative roles for TSPO. In 1999, Hardwick *et al.* observed that TSPO expression, nuclear localization, and TSPO-mediated cholesterol transport into the nucleus are involved in human breast cancer cell proliferation and aggressiveness [57]. Similarly, studies have shown that nuclear TSPO is associated with proliferative capacity of Erlich tumor cells [58]. Although the exact role of nuclear membrane cholesterol remains unknown, some propose it may be involved in the regulation of cell cycle related proteins, such as cyclin dependent kinases [59]. Together these studies suggest that nuclear TSPO can regulate the movement of cholesterol into the nuclear membrane and that this regulation is related to its modulation of cell proliferation.

1.4.6 Translocator Protein and Cancer

Numerous studies show increased TSPO expression in various malignancies, including those of the breast, prostate, colon, ovary, and endometrium [60-63]. A relationship between cell proliferation and TSPO expression has been observed in breast cancer cell lines [64]. Similarly, it has been reported that TSPO antagonists induce inhibition of cell proliferation in numerous *in vitro* models [60, 65-67]. In addition, it has been shown that TSPO overexpression correlates with the progression of breast, colorectal, and prostate cancers [68].

While prostate cancer was one of the first malignancies recognized to have elevated TSPO levels, few studies have examined the role of TSPO in neoplastic transformation of the prostate. Initial reports identified elevated expression of TSPO in R-3327 Dunning AT-1 prostate tumors [61]. Follow-up studies demonstrated that orchiectomized Dunning G rats had increased TSPO density in prostate tumors; altered expression was reversed following testosterone replacement [69], suggesting that TSPO expression may be regulated by androgens. More recently, immunohistochemical analysis has demonstrated significantly increased TSPO expression in human prostate cancer tissues when compared with benign prostatic hypertrophy and normal tissues [68]. However, despite these findings, few studies have investigated the role of TSPO in prostate cancer further.

1.5 PURPOSE

The rationale behind this research is 1) TSPO is elevated in human prostate cancer 2) TSPO antagonism inhibits prostate cancer cell growth and survival 3) TSPO multimers are believed to play a functional role in disease yet no one has investigated this further.

It is hypothesized that TSPO is a key factor involved in the progression to advanced prostate cancer through its actions as a regulator of apoptosis and cell proliferation. Our goal is to fully elucidate the changes that occur in TSPO in hormone refractory prostate cancer and determine how these changes impact disease development. The studies presented here are imperative in order to determine how changes in TSPO expression and form alter cellular function and examine the potential application of the TSPO antagonist, lorazepam, in cancer therapeutics.

1.6 MATERIALS AND METHODS

1.6.1 Cell Lines and Culture Conditions

Human prostate cancer cell lines PPC-1, LNCaP and DU145 (obtained from ATCC) were maintained in RPMI-1640 (Invitrogen; Grand Island, NY) supplemented with 10% fetal bovine serum (FBS) and 1% penicillin/streptomycin (P/S). LN05, LNCaP cells that have been deprived of androgens since 2005, was maintained in RPMI without phenol red with 10% charcoal

stripped FBS and 1% P/S. The human prostate cancer cell line LAPC4 (obtained from Dr. Rob Reiter, UCLA) was maintained in IMDM (Invitrogen) supplemented with 10% FBS and 1% P/S. LA98, the LAPC4 cell line deprived of androgens since 1998, was maintained in IMDM without phenol red (Invitrogen) supplemented with 10% charcoal stripped FBS and 1% P/S. Human embryonic kidney cells, HEK293 (obtained from ATCC), and human cervical cancer cells, HeLa (obtained from ATCC), were maintained in DMEM supplemented with 10% FBS and 1% P/S.

1.6.2 Tissue Microarrays and Immunocytochemistry

For these studies we used prostate tissue arrays (progression array, metastasis array and PSA failure array) from the in-house Western Pennsylvania Tumor Bank to directly compare TSPO staining intensity in the tissue specimens. Samples from benign kidney, breast, colon, testis and adrenal are included as positive and negative tissue controls for TSPO and are sampled in duplicate with sections at diagonally opposite ends of the block to eliminate positional staining artifacts.

There were 16 cases of normal donor prostates, 24 of non-neoplastic prostatic tissues adjacent to malignant glands (NAT), 24 of benign prostatic hyperplasia (BPH), 22 of prostatic intraepithelial neoplasia (PIN), 86 of prostatic adenocarcinoma (PCa), and 175 of metastatic prostate carcinoma (Met) from 35 patients with 25 separate sites of metastasis. Samples of benign testis and adrenal were also included on each TMA as positive controls for TSPO expression (n=2 each).

Immunohistochemical stains were performed on five-micron sections of TMA blocks. The sections of all the groups were deparaffinized and rehydrated through a graded series of

ethanol incubations. Heat induced epitope retrieval was performed using decloaker, followed by rinsing in TBS buffer for 5 minutes. Slides were then loaded on Dako Autostainer. The primary anti-TSPO antibody (working dilution 1:350) was a polyclonal rabbit antibody (Trevigen; Gaithersburg, MD). The immunolabeling procedures were carried out according to manufacturers' instruction using Dako Envision Labeled Polymer-HRP anti rabbit (Dako; Glostrup, Denmark). Slides were then counterstained in hematoxylin, step dehydrated and coverslipped. A prostate optimization MRA block was used as positive control for each antibody. Both the extent and intensity of immunopositivity were considered when scoring the expression of TSPO. Briefly, the intensity of positivity was scored from 0 to 3 as follows: 0 as non-stained, 1 as weak, 2 as moderate, and 3 as strong as positive control. The extent of positively stained cells was estimated using the same 0-3 scale. Semiquantitative analysis of TSPO expression in the human tissues were carried out in a blinded fashion by a board certified GU pathologist Dr. Anil Parwani using a 4-tier scoring method for intensity (0,1,2,3) added to percent expression in epithelia (intensity + (% x 3)). The final composite score was determined after adding the intensity and extent of positivity in the respective lesions.

1.6.3 Immunoblotting

TSPO

Human prostate cancer cells (PPC-1, DU145, LAPC4, LA98, LNCaP, LN05), HEK293, and HeLa cells were lysed in lysis buffer (20mM Tris-HCl, 135mM NaCl, 10% glycerol, and 1% Triton-X). Human hepatocyte lysate was obtained from Dr. Steven Strom, University of Pittsburgh and Jurkat cell lysate was obtained from Upstate (now Millipore; Billerica, MA).

Protein concentration was determined and an equal amount of protein (10 µg) was separated on 10% SDS-PAGE under reducing conditions. Proteins were electrotransferred onto PVDF membranes (Millipore; Billerica, MA) and blocked in 4% milk in PBST (PBS supplemented with 0.2% Tween20) for 1 hour at room temperature. Immunodetection of TSPO was carried out using the goat anti-TSPO polyclonal antibody (Novus Biologicals; Littleton, CO) at a dilution of 1:1000 at 4°C overnight. The membrane was washed in PBST and incubated with a donkey anti-goat secondary HRP-linked antibody (Santa Cruz Biotechnology; Santa Cruz, CA) at a dilution of 1:2000 for 1 hour at room temperature. Immunoreactivity was visualized using ECL (Amersham Life Sciences; Piscataway, NJ). Membranes were blotted for β-actin (Sigma Aldrich; St Louis, MO) at a dilution of 1:4000 as a control for protein loading.

Akt and p27

PPC-1 cells were plated at a density of 3×10^5 cells/well in 6-well plates. Cells adhered overnight and were then treated with TSPO antagonists PK11195 or lorazepam at 50µM. Protein was collected at the following time points: 0, 15m, 30m, 1hr, 2hr, and 4hr. Protein concentration was determined and an equal amount of protein (20 µg) was separated on 10% SDS-PAGE as described above. Immunodetection of Akt was carried out using the rabbit anti-pAKT and rabbit anti-AKT polyclonal antibodies (Cell Signaling; Davers, MA) at a dilution of 1:1000 at 4°C overnight. The membranes were washed in PBST and incubated with an anti-rabbit secondary HRP-linked antibody (Santa Cruz Biotechnology; Santa Cruz, CA) at a dilution of 1:2000 for 1 hour at room temperature. Immunoreactivity was visualized using ECL (Amersham Life Sciences). Membranes were blotted for β-actin (Sigma Aldrich) at a dilution of 1:4000 as a control for protein loading.

1.6.4 MTT Cell Viability Assay

PPC-1 human prostate cancer cells were plated at 5×10^3 cells/well in 96-well plates (Falcon-BD Biosciences; San Jose, CA) and adhered overnight at 37°C. The next day cells were treated with benzodiazepines lorazepam, estazolam, or temazepam (Sigma-Aldrich; St Louis, MO) or TSPO ligands PK11195 or Ro5-4864 (Sigma-Aldrich) at varying concentrations (0.1µM-100µM) or vehicle (EtOH or DMSO) for 48 hours at 37°C. The cells were then incubated for 4 hours with 3-(4,5-dimethylthiazol-2-yl)-2,5-diphenyl tetrasodium bromide (MTT) (Chemicon; Billerica, MA) according to the manufacturer's protocol. The optical density was measured at a wavelength of 570 nm using the SpectraMax M2^e absorption spectrophotometer (Molecular Devices; Sunnyvale, CA). This was repeated in three independent experiments.

1.6.5 Cell Proliferation Assay

PPC-1 and LN05 cells were plated at a density of 5×10^4 cells/well in 6-well plates. Cells adhered overnight and were then treated with TSPO antagonists PK11195 or lorazepam at 10µM, 50µM or 100µM or vehicle (EtOH or DMSO, respectively) for 72 hours. Cells were trypsinized and cell proliferation was measured by direct cell counting using a Coulter Counter (Beckman-Coulter; Fullerton, CA). This was repeated in three independent experiments.

1.6.6 Cell Death ELISA

LNCaP, LN05, and PPC-1 cells were plated at a density of 5×10^4 cells/well in 6-well plates. Cells adhered overnight and were then treated with TSPO antagonists PK11195 or lorazepam (PPC-1) at 10 μ M, 50 μ M or 100 μ M or vehicle (EtOH or DMSO, respectively) for 18 hours. A spectrophotometric apoptosis ELISA was used to quantify histone-associated DNA fragments present in the cell lysates according to manufacturer's instructions (Roche Diagnostics; Indianapolis, IN). Briefly, the standard solution and samples were added to the wells of a 96-well plate coated with a monoclonal antibody. After incubation, the plate was washed, and an enzyme-labeled antibody was added. After further incubation, the plate was washed again and treated with the substrate and the optical density was determined at 405 nm using the SpectraMax M2^e absorption spectrophotometer (Molecular Devices). This was repeated in three independent experiments.

1.6.7 Flow Cytometry for Annexin V Analysis

Human LNCaP and PPC-1 prostate cancer cells were plated in 100 mm plates and once cells reached approximately 70% confluence, cells were treated with 50 μ M or 100 μ M PK11195 TSPO antagonist or vehicle (EtOH) for 18 hours. For flow cytometry using the Annexin V assay, cells were collected and double-stained with fluorescein isothiocyanate-conjugated Annexin V (PharMingen; San Diego, CA) and propidium iodide (PI). Cells were counted and Annexin V was added according to the manufacturer's recommendations to 1×10^5 cells for each condition (in 100 μ l of Annexin V binding buffer) in duplicate with PI used at a final

concentration of 5 µg/ml. Annexin V positive cells were considered apoptotic and their percentage of the total number of cells was calculated. Cells taking up vital dye PI were considered dead. Samples of 10,000 cells were analyzed by FACScan flow cytometer with LYSIS II software package (Becton Dickinson).

1.6.8 Combination Therapy Studies

PPC-1 and LN05 cells were plated at 3×10^5 cells/well in 6-well plates. Cells adhered overnight and were then treated with docetaxel (1nM) or docetaxel plus varying concentrations of PK11195 or Lorazepam (1nM-100µM) for 48 hours. Cells were trypsinized and the number of cells was measured by direct cell counting using a Coulter Counter (Beckman-Coulter). This was repeated in three independent experiments.

1.6.9 TSPO Antagonism *in vivo*

PPC-1 cells were grown to 80% confluence in growth media. Cells were dissociated with trypsin, washed twice in Hank's balanced salt solution (HBSS) and 20 male athymic nu/nu mice (Charles River Laboratories; Wilmington, MA) received subcutaneous flank injections of 1×10^6 cells per 100 µl of HBSS. Mice were weighed and tumors were measured with calipers twice a week and tumor volumes were calculated (tumor volume = length x width x height x 0.5236). When the average tumor size reached approximately 100 mm^3 the mice were randomized into 2 groups (10 mice per arm) and given either lorazepam or vehicle (DMSO). Treatments were administered intraperitoneally at 40mg/kg lorazepam or vehicle (DMSO) 7 days a week for ~35 days. Once a

mouse's tumor burden reached 2 cm the mouse was sacrificed and the tumor was removed, weighed, fixed in 4% paraformaldehyde, and embedded in paraffin for analysis.

1.6.10 Immunohistochemistry

Five-micron sections of paraffin-embedded tumors were quenched in 3% hydrogen peroxide for 15 minutes and stained following citrate-steam antigen retrieval with TEC-3 Ki-67 (M7249; Dako, Carpinteria, CA) or PECAM (Santa Cruz Biotechnology) primary antibodies. A biotinylated secondary antibody was used, followed by streptavidin-conjugated horseradish peroxidase and 3,3'-diaminobenzidine chromogen (K0690; Dako). For labeling apoptotic nuclei, tissues were deparaffinized and treated with 0.3% H₂O₂ for 30 minutes to eliminate endogenous peroxidases. The DNA nick labeling reaction was carried out using 50U/ml Klenow (Roche Diagnostics), 2mM dNTP (Promega: Madison, WI) with 0.5nM biotin-16-dUTP (Roche Diagnostics) in buffer A (0.05M Tris, pH 7.5; 5mM MgCl₂; 0.058mM MESNA; and 0.05% bovine serum albumin) for 60 min at 37°C. The sections were then rinsed in PBS and incubated with 50mg/ml Peroxidase-Z-Avidin (Zymed Laboratories; San Francisco, CA) in PBS with 0.5% BSA for 30 min at 37°C. After rinsing, the labeling was visualized using a diaminobenzidine solution (90mg DAB (Sigma) in 150ml PBS, 600ul NiCl₂ + 60ul H₂O₂ 30%). As a positive control, adjacent tissue sections were treated with DNaseI (0.1 mg/ml). All of the tissues were scored in a blinded fashion by 2 independent observers.

1.6.11 Tumor Growth Modeling

A nonlinear mixed effects approach to examine tumor growth longitudinally was implemented to describe the growth characteristics of the PPC-1 cells under vehicle and lorazepam treated arms. This was done using the NONMEM V 1.1 (Icon development solutions, Ellicott City MD USA). Specifically, the nonlinear mixed effects approach allowed the data to be probed with respect to both the shape of the growth curves, with exponential, gompertz and logistic models tested and compared using the Akaike Information Criterion (AIC). The mean PPC-1 cell volume was used for the calculations ($3.43 \pm 0.03 \mu\text{m}^3$). The Gompertz Model provided the best fit:

$$y = Base + \alpha \times \exp^{-2.718^{-\kappa \times (time - \gamma)}}$$

1.6.12 Stable Transfections

TSPO overexpression

A vector containing TSPO cDNA (pCMV6-TSPO) was purchased from Origene (Rockville, MD) and the empty vector was used as a negative control for all experiments. HEK293 cells were transfected using Lipofectamine (Invitrogen; Carlsbad, CA), stable clones selected by neomycin resistance and TSPO expression levels were analyzed by immunoblot analysis as described above. The HEK293 cells overexpressing TSPO will be referred to as HEK293 TSPO.

TSPO knockdown

Four shRNA directed against TSPO were purchased from SABiosciences (Frederick, MD) and screened for TSPO knockdown. The TSPO shRNA (GAGCAGTGTCTGTGCTTTCT)

demonstrated the most efficient knockdown and therefore used in the subsequent experiments. A nonsense shRNA construct was used as a negative control for all experiments. PPC-1 cells were transfected using Lipofectamine (Invitrogen; Carlsbad, CA), stable clones selected by neomycin resistance and TSPO expression levels were analyzed by immunoblot analysis as described above. PPC-1 TSPO knockdown cells will be referred to as PPC-1 shTSPO and control cells PPC-1 NC.

1.6.13 Susceptibility to Lorazepam and Cell Proliferation

TSPO Overexpression

HEK293 and HEK293 TSPO cells were plated at a density of 3×10^5 cells/well in 6-well plates. Cells adhered overnight and were then treated with 50 μ M lorazepam for 48 hours. Following treatment, cells were trypsinized and counted using a Coulter Counter. This was repeated in three independent experiments.

HEK293 and HEK293 TSPO cells were plated at a density of 5×10^4 cells/well in 6-well plates and adhered overnight. Cell counts were done each day for 3 days using a Coulter Counter. This was repeated in three independent experiments.

TSPO Knockdown

PPC-1 NC and PPC-1 shTSPO Y1 and Y2 cells were plated at a density of 3×10^5 cells/well in 6-well plates. Cells adhered overnight and were then treated with 50 μ M lorazepam for 48 hours.

Following treatment, cells were trypsinized and counted using a Coulter Counter. This was repeated in three independent experiments.

PPC-1 NC and PPC-1 shTSPO Y1 and Y2 cells were plated at 5×10^3 cells/well in triplicate in a 24-well dish in regular growth medium and adhere overnight. Cells were washed once with PBS and serum free medium was added and the cells incubated for 24 hours in order to arrest the cell cycle. The following day $1\mu\text{Ci/ml}$ ^{14}C -Thymidine (Amersham 50Ci/ml) was added in regular growth medium and incubated for 16 hours. Cells were washed twice in ice-cold PBS then incubated with 10% trichloro acetic acid for 5 mins on ice. Cells were solubilized by adding 500uL 1N NaOH. Radioactivity was quantified using Wallac 1470 Gamma Counter (Perkin Elmer Life Sciences; Turku, Finland). This was repeated in three independent experiments.

1.6.15 Colony Formation Assay

PPC-1 NC and PPC-1 shTSPO Y1 and Y2 cells were plated at a density of 2×10^3 cells/well in duplicate in 100mm dishes. Cells adhered overnight and were then treated with $50\mu\text{M}$ or $100\mu\text{M}$ lorazepam for 72 hours. Regular growth medium was replaced and the cells grew at 37°C for 14 days. Cells were stained with 0.01% crystal violet in 20% MeOH and individual colonies were blindly counted by 2 different observers. This was repeated in three independent experiments.

1.6.16 Wound Healing Assay

PPC-1 NC and PPC-1 shTSPO Y1 and Y2 cells were plated in triplicate in regular growth medium and grown to confluence in a 24-well dish. Scratches were made using a 200 μ l pipette tip and cells were washed twice in PBS to remove detached cells. Three pictures of each well were taken at 0 and 24 hour time points. This was repeated in three independent experiments.

1.6.17 Soft Agar Colony Formation Assay

To make the bottom layer of agar, 1ml of regular growth medium was added to 1 ml 1.2% BactoAgar for each well. PPC-1 NC and PPC-1 shTSPO Y1 and Y2 cells were plated in triplicate at 1×10^4 cells/well in 6-well plates in 1.5ml regular growth medium added to 0.5ml 1.2% BactoAgar and incubated at 37°C for 14 days. Individual colonies were counted in 4 different fields at a magnification of 4x using a light microscope. This was repeated in 3 independent experiments.

1.6.18 Matrigel Invasion Assay

BD BioCoat™ Matrigel™ Invasion Chambers and Control Cell Culture Inserts (BD Biosciences; San Jose, CA) were purchased and rehydrated in 500 μ l serum free medium (RPMI) for 2 hours at 37°C. PPC-1 NC and PPC-1 shTSPO Y1 and Y2 cells were trypsinized and reconstituted at 2×10^4 cells/ml in 0.5% FBS containing media. After rehydration, media was aspirated from the wells and inserts and 500 μ l of 10% FBS RPMI was added to the wells and 500 μ l of cells were

added to the insert (for a total number of cells plated of 1×10^4) and incubated at 37°C for 20 hours. The next day, media was removed from the inserts and the matrigel surface was “scrubbed” with a moist Q-tip to remove any non-invading cells. Each insert was placed into 500ul MeOH + 0.1% crystal violet for 5 mins to fix and stain the cells. Inserts were then washed in H₂O four times and dried at room temperature for 2 hours. The number of cells that migrated through the control inserts and those that invaded through the matrigel were counted at a magnification of 10x using a light microscope.

1.6.19 Mouse and Human Tissue

Mouse tissues were obtained from the Transgenic Adenocarcinoma of Mouse Prostate (TRAMP) model of prostate cancer. This model uses the rat probasin promoter to directly express SV40 early genes to prostate epithelium. Male TRAMP mice exhibit consistent prostate-specific patterns of expression and develop prostatic intraepithelial neoplasia that becomes invasive and metastasizes primarily to the lymph nodes and lungs. Prostate, lymph nodes, and lung tissue were examined for these studies. Human tissue was obtained from the Health Sciences Tissue Bank at the University of Pittsburgh. Primary prostate cancer and prostate cancer lymph node metastases were examined for these studies.

1.6.20 Transient TSPO Knockdown

Short-interfering RNA (siRNA) directed against TSPO (5' CACUCAACUACUGCGUAUG 3') or scrambled siRNA (Sigma) were transiently transfected into PPC-1 human prostate cancer cells

using Lipofectamine 2000 (Invitrogen) at approximately 90% confluence. Cells were collected each day for 8 days and protein was extracted for western blot analysis using the Novus antibody against TSPO that was previously described in Methods 1.6.3.

1.6.21 Breaking Di-Tyrosine Bonds

PPC-1 human prostate cancer cell lysates were treated with 8M Urea, an agent previously described to break di-tyrosine bonds, for 1, 4, 6, 8, or 24 hours. Cells were collected and protein was extracted for western blot analysis using the Novus antibody against TSPO that was previously described in Methods 1.6.3.

1.6.22 Forming Di-Tyrosine Bonds

PPC-1

PPC-1 human prostate cancer cells were collected and lysed. Lysates (20ug) were treated with 1, 10, or 100 μ M hydrogen peroxide (H₂O₂), a source of reactive oxygen species, for 16 or 24 hours at 37°C. Lysates were run on a 10% SDS-PAGE gel and immunoblot analysis was performed using the Novus antibody against TSPO that was previously described in Methods 1.6.3.

MLL

The rat prostate cancer cell line, MatLyLu (MLL,) was utilized for these studies because it lacks the endogenous 18kDa TSPO. MLL cells were transfected with a vector containing TSPO

cDNA (pCMV6-TSPO) (Origene). These cells will be referred to as MLL TSPO. Lysates from MLL TSPO cells were collected, treated with H₂O₂, and screened as described above.

1.6.23 Reactive Oxygen Species Scavenger Studies

Reactive oxygen species (ROS) have been implicated in di-tyrosine bond formation in TSPO. PPC-1, MLL, and MLL TSPO clones 4 and 5 were treated with varying concentrations of ROS scavengers N-acetylcysteine, Vitamin C, Trolox, and Catalase (Sigma) for 8, 24, or 48 hours. Cells were collected, lysed, and protein was extracted for western blot analysis using the Novus antibody against TSPO that was previously described in Methods 1.6.3.

1.6.24 Targeting a Tyrosine in TSPO for Site-Directed Mutagenesis

In order to determine if tyrosine bond formation was responsible for the higher molecular weight bands, mutations to the tyrosines present in the TSPO protein sequence would be necessary. The expertise of structural biologist Dr. Judith Klein-Seetharaman of the University of Pittsburgh was utilized to make an educated deduction as to which of the ten tyrosines to target first. Using a process of elimination, it was decided that the tyrosine located at amino acid 34 is the most likely candidate based on its cellular availability and is highly conserved in nature among almost all species examined.

1.6.25 TSPO Construct Generation and Transfection

The vector containing TSPO cDNA (pCMV6-TSPO) (Origene) was sent to GenScript (Piscataway, NJ) for site-directed mutagenesis of the tyrosine located at amino acid 34 of TSPO to phenylalanine. This construct will be referred to as TSPO SDM Y-F. The TSPO SDM Y-F construct was transfected into PPC-1, HEK293, and MLL cells using Lipofectamine (Invitrogen). TSPO expression was screened 72 hours post-transfection.

1.6.26 Reactive Oxygen Species Inducer and Multimer Formation

HEK293 and MLL cells transiently expressing the TSPO SDM Y-F construct were treated with the reactive oxygen species generating enzyme glucose oxidase at 1, 0.5, 0.1, .05, and .01 units/ml for 6 hours at 37°C. Cells were collected and protein was extracted for western blot analysis using the Novus antibody against TSPO that was previously described in Methods 1.6.3.

2.0 TSPO AS A REGULATOR OF CELL PROLIFERATION AND APOPTOSIS IN PROSTATE CANCER

2.1 INTRODUCTION

The predictable pattern of progression in hormone-refractory prostate cancer, coupled with its plodding growth rate produces a large window for meaningful intervention, yet no therapy exists that reliably cures this form of the disease. As a particularly slow-growing disease, prostate cancer does not typically respond well to chemotherapy; thus, new therapeutic strategies are critical.

Translocator Protein (TSPO), previously known as the peripheral benzodiazepine receptor, is a transmembrane molecule that is best known for transporting cholesterol across the mitochondrial membrane for cell signaling and steroid biosynthesis [35, 45]. TSPO has been shown to be overexpressed in numerous malignancies, including those of the breast, prostate, colon, ovary, and endometrium [60, 62, 70-72]. Furthermore, a correlation has been drawn between TSPO overexpression and the progression of breast, colorectal, and prostate cancers [68]. Functionally, it is suggested that TSPO takes part in the regulation of apoptosis through its interactions with the mitochondrial permeability transition pore [50, 73]. Studies have shown that

treatment of cancer cells with the TSPO antagonist PK11195 results in cell death [52-54, 65]. TSPO also plays a role in cell proliferation, as a correlation between TSPO expression and cancer cell proliferation has been observed in human astrocytomas [74] and breast cancer [75] while TSPO antagonism inhibits cell proliferation [66, 67, 76, 77]. In addition, studies have shown that TSPO inhibition results in cell cycle arrest in numerous cancer models. [50, 52, 60, 66, 78].

Initial reports identified elevated expression of TSPO in rat R-3327 Dunning AT-1 prostate tumors [70]. Follow-up studies demonstrated that orchietomized Dunning rats with Dunning G tumors also had increased TSPO density in prostate tumors; however, treatment with testosterone repressed TSPO ligand binding, suggesting a role for testosterone in TSPO expression levels in these hormone-sensitive prostatic tumors [79]. TSPO density is decreased in the male genital tract but not the heart after castration, indicating TSPO levels are affected in organs regulated by the trophic influence of testosterone [80]. While downregulation of TSPO during androgen depletion occurs in normal male rat urogenital tissues, the receptor is upregulated in genitourinary cancer cells with androgen withdrawal. Immunohistochemical studies found significantly increased TSPO expression in human prostate cancer tissues when compared with benign prostatic hyperplasia and normal tissues [68]. However, despite these promising findings, few studies have investigated the role of TSPO in prostate cancer further.

In this study, the goals were to 1) verify the expression profile of TSPO in human prostate cancer 2) determine the functional effects of modulating TSPO using pharmacologic agents targeting TSPO and 3) investigate the therapeutic potential of lorazepam for advanced prostate cancer.

2.2 RESULTS

2.2.1 TSPO expression is increased in human prostate cancer.

To determine relative expression levels of TSPO in human tissue, we performed immunohistochemical analysis of prostate cancer tissue microarrays [81]. As shown in Figure 4A & B-G, we observe significantly increased expression of TSPO in prostatic intraepithelial neoplasia (average score: 3.0/6), primary prostate cancer (4.1/6), and prostate cancer metastases (4.8/6) compared to normal donor (2.0/6), normal tissue adjacent to tumor (2.1/6), and benign prostatic hyperplasia (1.8/6). Furthermore, TSPO expression increases with progression, as prostate cancer metastases have the highest expression levels. Testes and adrenals are steroidogenic tissues documented as having relatively high TSPO expression and were therefore used as positive controls.

Increased expression of TSPO is also observed *in vitro* with elevated expression in prostate cancer cell lines PPC-1, DU145, LAPC4, LA98, LNCaP, and LN05 compared to the human embryonic kidney cell line (HEK293), T lymphocytes (Jurkat), a tumorigenic cervical cancer cell line (HeLa), and human hepatocytes (Hep) (Figure 5). It is important to note that the 36kDa band observed is not unique to these studies, as higher molecular weight bands have previously been reported in western blots using antibodies against TSPO [82, 83].

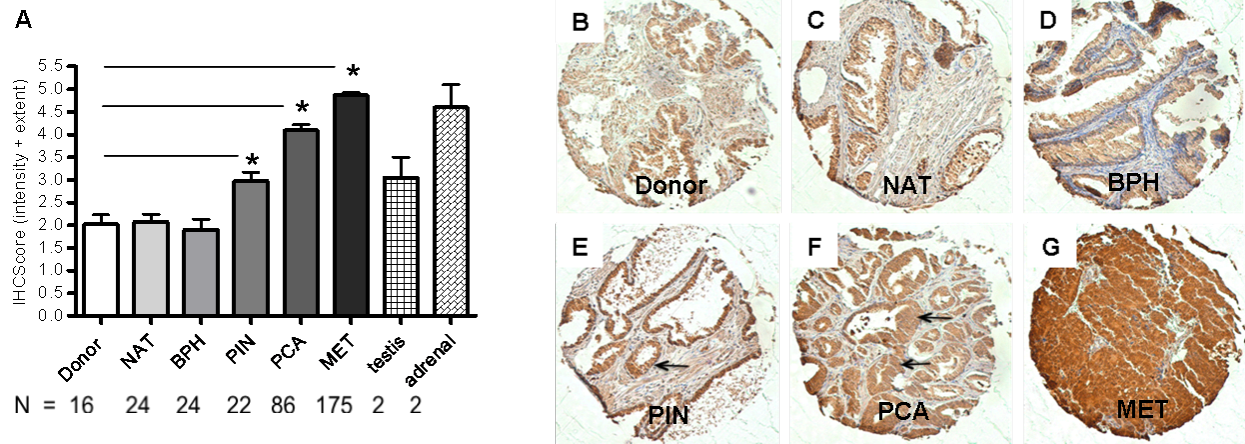


Figure 4. TSPO expression is increased in human prostate cancer tissues.

(A) relative expression of TSPO by immunohistochemistry (IHC) in normal donor prostate (donor), normal prostate tissue adjacent to tumor (NAT), benign prostatic hyperplasia (BPH), prostatic intraepithelial neoplasia (PIN), primary prostate cancer (PCA), and prostate cancer metastases (MET) by scoring of TMA cores. (B-G) Representative results of TSPO staining in normal donor prostate (B) NAT (C), BPH (D), PIN (E), PCa (F), and PCa metastasis (G). Arrow indicates PIN and primary prostate cancer glands. * indicates statistical significance $p < 0.05$

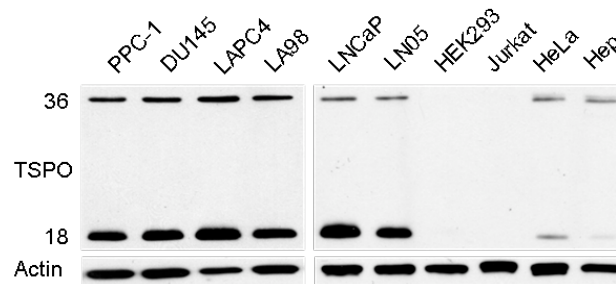


Figure 5. TSPO expression is increased in human prostate cancer cell lines.

TSPO expression in human prostate cancer cell lines PPC-1, DU145, LAPC4, LA98, and LNCaP, LN05 compared to human embryonic kidney cells (HEK293), human T lymphocytes (Jurkat), human cervical cancer cells (HeLa), and human liver hepatocytes (Hep).

Gleason grading is a way to score prostate cancer tissue based on the architecture of the cancerous prostate glands. The Gleason grading scale ranges from very well differentiated cells (grade 1) to very poorly differentiated (grade 5). Two different Gleason grades are assigned to the tissue, representing the primary tissue structure and the secondary tissue structure, for a

Gleason score ranging from a possible 2 (1+1) up to 10 (5+5). Analyses of prostate tumor Gleason sum and stage were carried out to identify whether TSPO is altered with disease progression. TSPO levels were high in all tumor specimens compared to normal adjacent glands and TSPO expression increased with increasing grade and stage in the TMA specimens (Table 1). TSPO levels in adenocarcinoma were significantly higher than PIN or NAT when matched for stage except in stage II specimens in which PIN regions demonstrated TSPO levels equivalent to regions of NAT. There was also a significant change in TSPO levels with Gleason sum. High TSPO levels are evident in Gleason ≤ 6 (4.02 ± 0.93) samples compared to the adjacent normal glands (NAT; 2.44 ± 0.63) and increased with Gleason sums 7 (4.16 ± 0.95), Gleason 8 (4.48 ± 0.90) and Gleason 9 (4.58 ± 1.11).

PSA failure is defined as a rise of PSA in the serum following treatment with surgery or radiation. Assessment of TSPO expression in the PSA failure array shows a significant difference in the NAT glands of patients with PSA failure compared with the NAT of patients who remain disease free (Table 1). However there was no difference in the PIN or adenocarcinoma expression of TSPO in the primary tumors of patients with PSA failure compared to disease free patients. The PSA failure array did not contain specimens from patients that have remained disease free, so the samples on the progression array were used for this comparison and matching control tissue was used as comparison between TMAs to assure IHC scoring remained the same across separate arrays.

Table 1. TSPO immunostaining in human prostate tissue by Gleason, stage and PSA failure.

Gleason		<6	7	8	9
		4.02 ±0.93 (n=39)	4.16 ±0.95 (n=81)	4.48 ±0.90 (n=42)	4.58 ±1.11* (n=25)
Stage		PCa	PIN	NAT	
	II	3.97 ±0.86 (n= 19)	3.01 ±1.06 (n = 15)	2.85 ±0.92 (n= 18)	
	III	4.14 ±1.04 (n= 59)	3.52 ±0.95 (n = 19)	2.58 ±0.93 (n = 32)	
	IV	4.46 ±0.88* (n = 23)	3.63 ±0.51 (n = 3)	2.65 ±0.79 (n = 19)	
PSA failure		4.17 ±0.97 (n=50)	3.34 ±0.98 (n=19)	2.66 ±0.88* (n=35)	
disease free		4.02 ±1.13 (n=78)	2.91 ±0.75 (n=17)	2.07±0.82 (n = 23)	

* indicates statistical significance <0.05. Gleason 9 specimens showed higher TSPO levels than Gleason sum 6 and 7 but not Gleason 8. Stage IV PCa had higher TSPO than both stage II and III tumors.

2.2.2 TSPO antagonism has anti-proliferative and pro-apoptotic effects *in vitro*.

We began our preliminary functional studies to identify cancer cell sensitivity to TSPO receptor blockade by screening a series of potential TSPO antagonists, including benzodiazepines temazepam, lorazepam, estazolam, and Ro5-4864, and the isoquinoline carboxamide PK11195. To examine the antagonistic effects of these compounds on cell viability, PPC-1 human prostate cancer cells were treated with these drugs at varying concentrations (0.1-100µM). Among all of the compounds examined, the benzodiazepine lorazepam and PK11195 demonstrated the most significant antagonistic properties (Figure 6). Additionally, the effect of these TSPO ligands on cell proliferation was examined and a decrease in cell number following treatment with either PK11195 or lorazepam was observed (Figure 7).

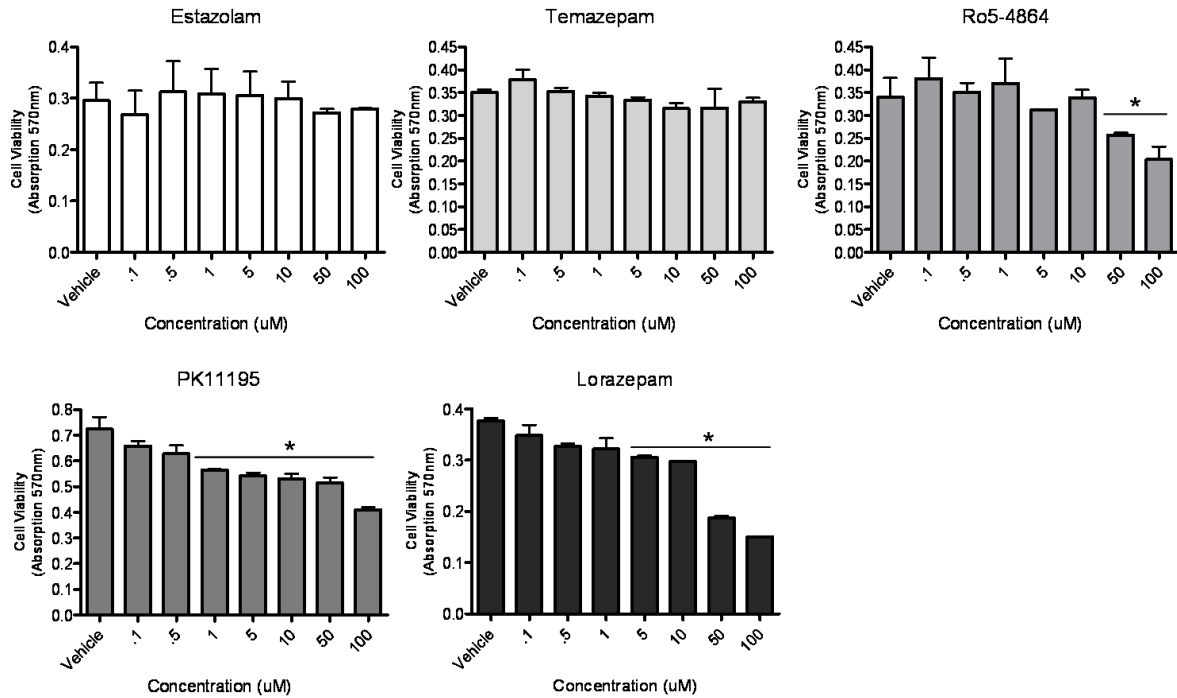


Figure 6. TSPO antagonism decreases cell viability in prostate cancer cells *in vitro*.

MTT assay following 48 hour treatment of PPC-1 with PK11195 or Lorazepam. * indicates statistical significance $p < 0.05$

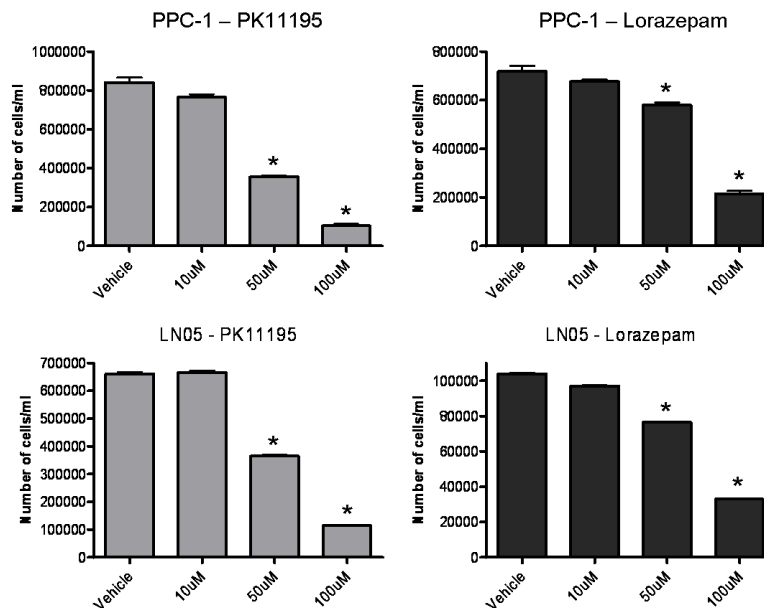
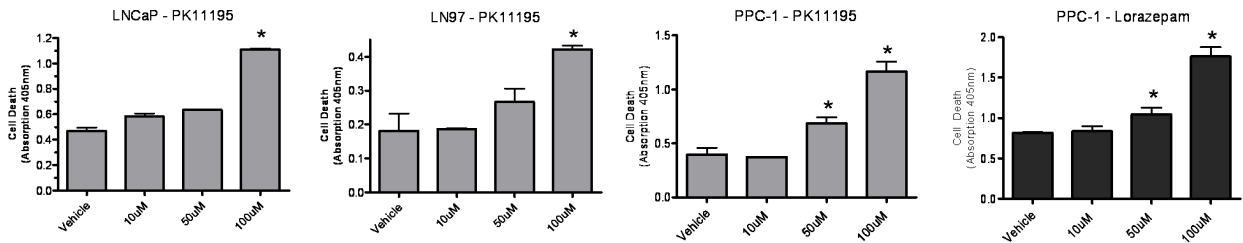


Figure 7. TSPO antagonism decreases cell proliferation in prostate cancer cells *in vitro*.

Direct cell counting of PPC-1 and LN05 cells treated with varying concentrations of PK11195 or Lorazepam or vehicle for 48 hours. * indicates statistical significance $p < 0.05$

In other cancer *in vitro* models, TSPO antagonists have been shown to reduce cell survival through apoptosis. The next experiment was to determine whether the decrease in cell proliferation with treatment with PK11195 or lorazepam was actually due to an induction of apoptosis. PPC-1 cells treated with PK11195 or lorazepam demonstrated a dose-dependent increase in apoptosis following treatment with PK11195 or lorazepam, while LNCaP and LN97 cells only showed significant apoptotic induction at the highest concentration of PK11195 (100 μ M) (Figure 8A). Using Annexin V staining and flow cytometry, a dose-dependent increase in apoptosis in PPC-1 cells treated with PK11195 was also observed (Figure 8B).

A.



B.

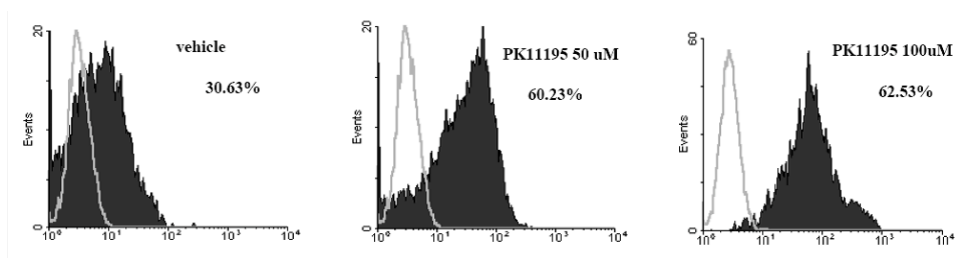


Figure 8. TSPO antagonism increases apoptosis in prostate cancer cells *in vitro*. A. Cell death ELISA following 18 hour treatment with varying concentrations of PK11195 or Lorazepam or vehicle. B. Annexin V based flow cytometry of PPC-1 cells treated with PK11195. * indicates statistical significance $p < 0.05$

2.2.3 TSPO Antagonism Modulates Survival and Cell Cycle Related Proteins

The next goal was to elucidate the cellular signaling pathway by which TSPO ligands were exhibiting their anti-survival and anti-proliferative effects. In a time dependent manner, 50 μ M PK11195 and lorazepam decreased phosphorylation of Akt (pAkt), a protein that is well characterized for its role in cell survival. Lorazepam showed a quicker response, decreasing pAkt levels as early as 15 minutes after treatment (Figure 9).

The expression status of the cell cycle inhibitor p27 was also investigated. Figure 9 demonstrates an increase in p27 expression 1 hour after treatment with either PK11195 or lorazepam. Interestingly, p27 levels in PK11195 treated cells went back down to baseline at 4 hours, while p27 levels in lorazepam treated cells remained elevated.

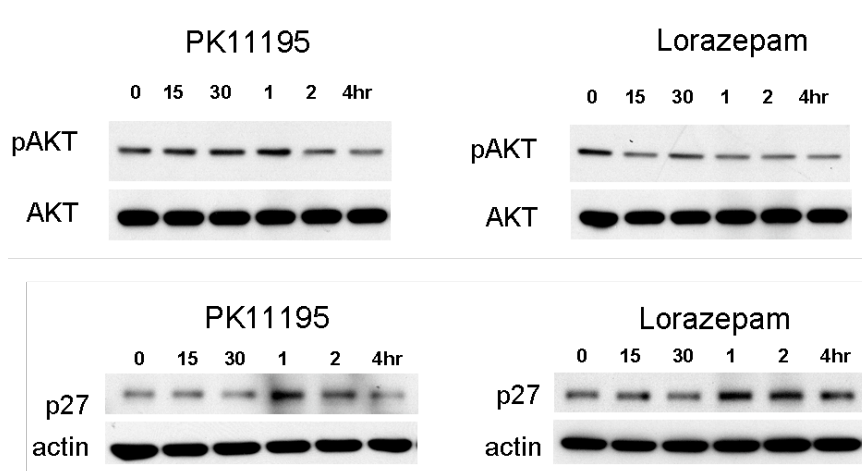


Figure 9. Time course decrease of pAkt and induction of p27 expression by TSPO antagonism.

Immunoblots were reprobbed for total Akt (to ensure that treatment with TSPO ligands did not affect total Akt levels) or B-actin (to ensure equal loading). Data are representative of three independent experiments.

2.2.4 *In vitro* analysis of combination TSPO antagonism and Taxotere (docetaxel) treatment in prostate cancer cells.

Docetaxel is a cytotoxic agent that binds to the B subunit of tubulin, resulting in irreversible polymerization of microtubules. Stabilization of microtubules, which comprise the mitotic spindles, effectively paralyzes the cell in mitosis, leading to the initiation of the apoptotic cascade. Using direct cell counting, the question of whether PK11195 or lorazepam could enhance the cellular response to docetaxel was tested. Studies have suggested that TSPO antagonists may modulate the Akt survival pathway as well as promote opening of the mitochondrial permeability transition pore, the critical step in apoptosis induction. Therefore, we believe that there may be an enhanced effect when TSPO antagonists are combined with Docetaxel. PPC-1 and LN05 cells were treated with 1) vehicle 2) 1nM docetaxel or 3) 1nM docetaxel and PK11195 (or lorazepam) at varying concentrations (1nM-100 μ M) for 48 hours. Figure 10 demonstrates a significant combinatorial effect of docetaxel plus PK11195 but not docetaxel plus lorazepam (compare to Figure 6).

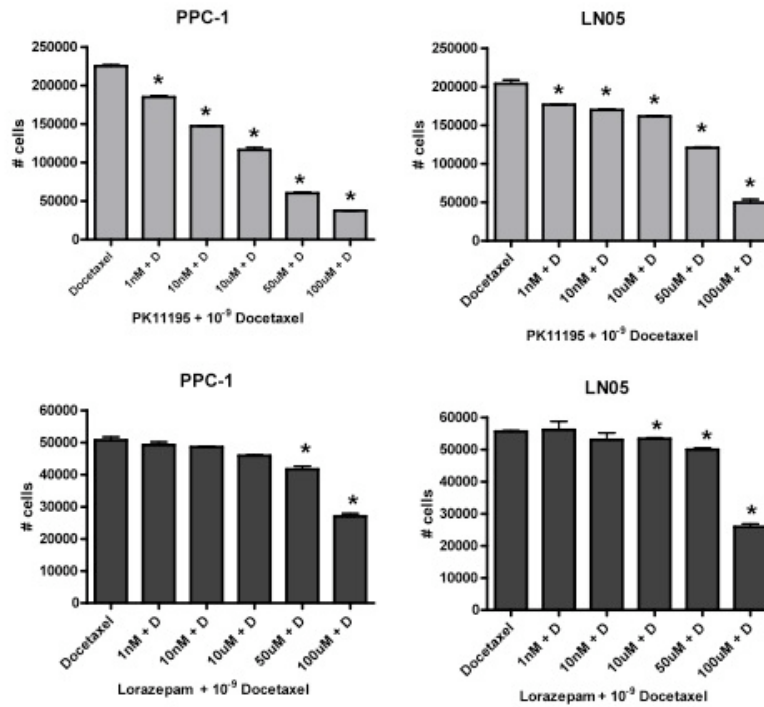


Figure 10. Effect of combination docetaxel + PK11195/lorazepam on prostate cancer cell growth.

Direct cell counting of cells treated with docetaxel alone or docetaxel + PK11195/lorazepam

D: docetaxel (10^{-9}) * indicates statistical significance $p < 0.05$

2.2.5 TSPO Antagonism has Anti-Proliferative and Pro-Apoptotic Effects *In Vivo*.

To examine the *in vivo* efficacy of TSPO inhibition, 20 athymic male mice received subcutaneous flank injections of prostate cancer cells. When tumors reached $\sim 100\text{-}200 \text{ mm}^3$, the mice were randomized into two treatment groups (10 mice per arm) such that each mouse received a daily dose of either 40 mg/kg lorazepam or vehicle (1% DMSO). Tumor measurements were recorded twice a week and mice were euthanized when tumors dimensions reached 2 cm. The tumor measurements demonstrate a divergence in tumor growth between lorazepam and vehicle treated mice: by week nine, lorazepam treated mice exhibited a

significantly smaller average tumor volume ($2682 \pm 539 \text{ mm}^3$) when compared to vehicle treated mice ($7392 \pm 346 \text{ mm}^3$) (Figure 11).

A nonlinear mixed effects approach to examine tumor growth longitudinally was implemented to describe the growth characteristics of the PPC-1 cells under vehicle and lorazepam treated arms. The gompertz model resulted in the lowest AIC and objective function values by approximately 25 points under the FOCE Interaction estimation method ($p < 0.001$ for the objective function with 2df). Individually, treatment groups were distinguishable with a covariate representing lorazepam treatment for the kappa (growth rate), gamma (time of maximum growth) and alpha (maximum tumor size) terms ($p < 0.001$) individually. However, once multiple factors were added, the effect of treatment on the alpha term (i.e., the projected maximum size asymptote for the tumor) was greatest, and the effect on the other two terms were no longer significant. Specifically, the objective function changed from 1791.3 to 1728.8 with the addition of lorazepam treatment as a covariate on the alpha term. This represents a statistically significant change with $p < 0.0001$ for 1 degree of freedom. In addition, the presence of lorazepam resulted in a predicted maximum tumor size approximately $\frac{1}{2}$ as large as that predicted in the presence of vehicle (14900 vs 28400um^3).

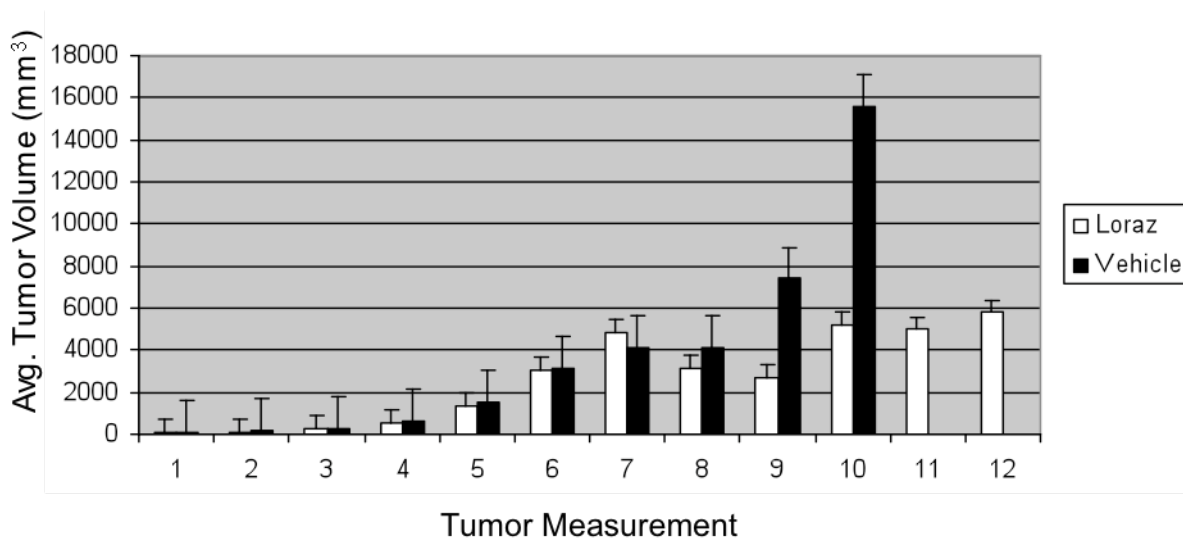


Figure 11. TSPO antagonism decreases average prostate cancer tumor volume over time.

Average tumor volume over time of athymic nude mice bearing PPC-1 xenograft tumors treated daily with Lorazepam (40mg/kg) or 1% DMSO. Tumor volume was measured twice weekly as described in the Materials and Methods section.

Once the tumor burden reached 2 cm, the mice were sacrificed 2 hours after the last dose of vehicle or lorazepam, and tumors were removed and processed for analysis. Tissue sections were stained for TSPO to determine if lorazepam treatment altered TSPO density [84, 85]. Lorazepam had an effect on cell proliferation, as there was a significant decrease in expression of the proliferation-associated protein Ki67 in mice treated with lorazepam compared to the vehicle group (Figure 12). Furthermore, lorazepam treatment did not affect vascularization, as the number of vessels per field was not significantly different between the two groups (Figure 12). TUNEL analysis reveals that lorazepam has pro-apoptotic actions *in vivo*, with the lorazepam treated group having significantly more apoptotic cells compared to the vehicle group (Figure 12).

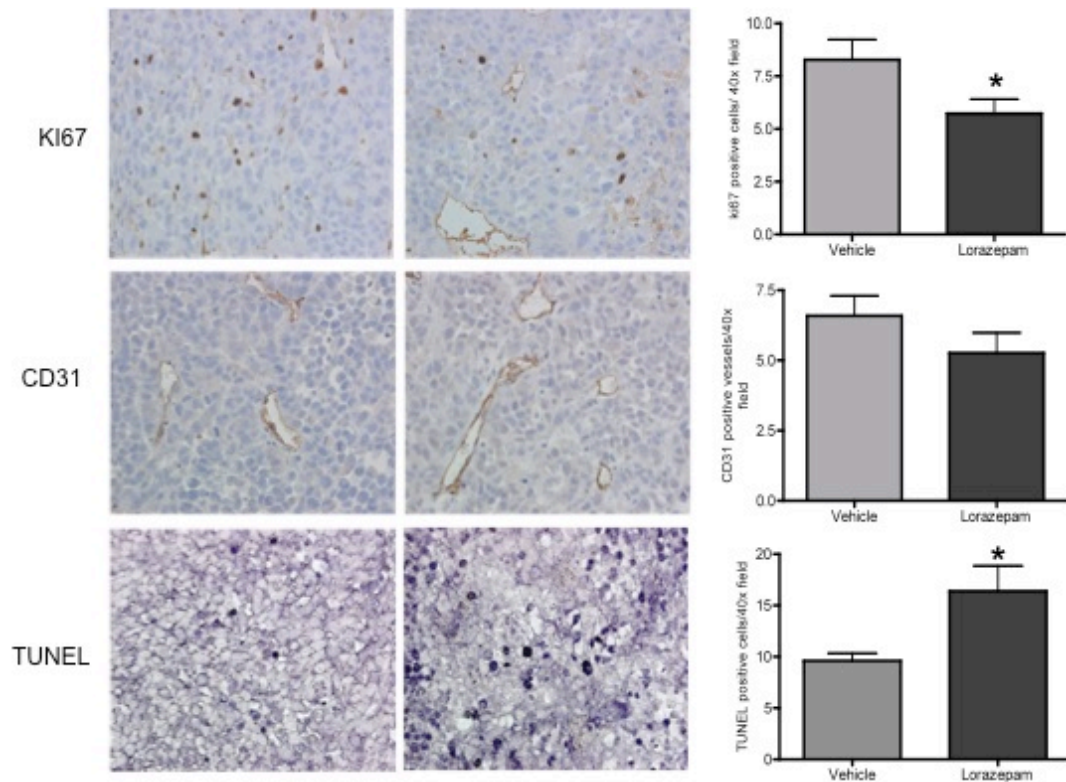


Figure 12. TSPO antagonism decreases cell proliferation and increases apoptosis in prostate cancer cells *in vivo*.

Immunohistochemical staining of lorazepam or vehicle treated PPC-1 xenograft tumors for cell proliferation (Ki67), microvascular density (CD31), and apoptosis (TUNEL). Bars graphs represent average values of positive signal counted in four random fields (40X magnification) * indicates statistical significance $p < 0.05$

2.3 CONCLUSIONS

In this series of experiments it was shown that TSPO expression is increased in human prostate cancer. Furthermore, TSPO expression appears to increase with disease progression, as the prostate cancer metastases have the highest expression levels. TSPO is also highly expressed in

prostate cancer cell lines, regardless of their androgen-sensitivity. These data support previous reports that TSPO expression is elevated in numerous cancer models, including prostate.

The *in vitro* TSPO antagonism studies presented here reveal that TSPO functions similarly in prostate cancer as it does in previously reported cancer models. Through pharmacologic inhibition, it was shown that TSPO can regulate critical cellular processes involved in transformation such as cell proliferation, cell survival, and cell death. Further studies are required to fully elucidate the molecular mechanisms by which these TSPO ligands are exhibiting their antagonistic effects.

The prostate cancer xenograft mouse study using lorazepam showed for the first time the anti-cancer properties of a benzodiazepine *in vivo*. The effect that lorazepam had on tumor growth over time was quite significant, reducing the tumor volume to half of the size of the vehicle treated tumors. Additionally, immunohistochemistry revealed that lorazepam exhibited similar anti-proliferative and pro-apoptotic properties *in vivo* as it did *in vitro*, evidenced by the decrease in the proliferative marker Ki67 and increase in TUNEL staining, indicative of an increase in cell death. Together, these studies provide additional insight into the role of TSPO as a modulator of apoptosis and proliferation, providing further evidence for its role as a potential therapeutic target for prostate cancer.

3.0 THE EFFECTS OF MODULATING TSPO EXPRESSION IN PROSTATE CANCER

3.1 INTRODUCTION

Numerous studies have suggested a correlation between TSPO overexpression and cancer aggressiveness. For example, TSPO overexpression was found to be a prognostic indicator of the aggressive phenotype in breast, colorectal, and prostate cancers [65]. In addition, Rechichi *et al.* showed that increasing TSPO in glioma cells resulted in an increase in motility, transmigration, and proliferation [86]. The human TSPO expression analysis previously presented here suggests that TSPO levels increase with aggression as prostatic intrapithelia neoplasia (PIN) had relatively low expression, primary prostate cancer had an intermediate level of expression, and prostate cancer metastases had the highest levels of expression (see Figure 4). Collectively these studies suggest that TSPO may play a role in progression of cancer. The studies presented in this chapter investigate the effects of modulating TSPO expression, both increasing and decreasing, on cellular phenotypes associated with advanced disease.

3.2 RESULTS

3.2.1 TSPO overexpression in HEK293 human kidney cells.

Figure 13 shows the drastic increase in TSPO expression (18kDa only) in HEK293 cells transfected with full length TSPO. HEK293 cells overexpressing TSPO will be referred to as 293-TSPO A/B and the empty vector control 293-C.

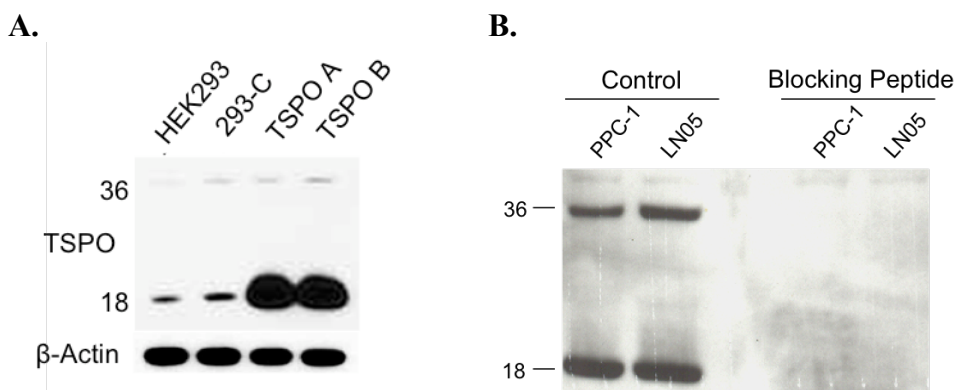


Figure 13. TSPO overexpression in HEK293 cells and TSPO antibody specificity.

A) 293-C: empty vector control, TSPO A/B: HEK293 cells overexpressing TSPO. Immunoblots were reprobed for B-Actin to ensure equal loading. B) Peptide competition assay showing specificity of the TSPO Novus antibody in two human prostate cancer cell line lysates, PPC-1 and LN05.

3.2.2 The effect of TSPO overexpression on susceptibility to lorazepam.

Overexpression of TSPO in HEK293 cells (Figure 13) significantly increased susceptibility of the cells to TSPO antagonism (Figure 14). HEK293-TSPO cells and wild-type HEK293 cells

were treated with 50 μ M lorazepam and cell counts analyzed after 48 hrs. Lorazepam significantly reduced cell numbers in 293-TSPO cells but not in the controls (Figure 14).

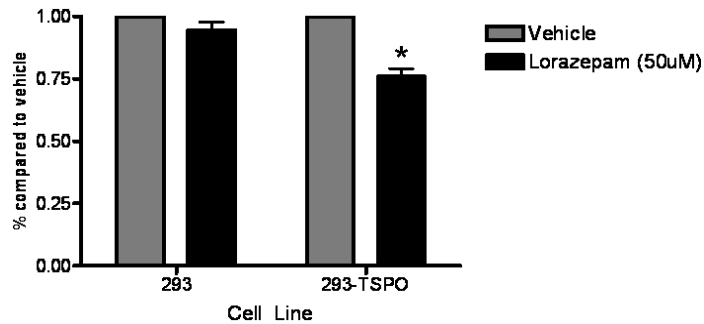


Figure 14. TSPO overexpression increases susceptibility to lorazepam in HEK293 cells.

Direct cell counting of 293 and 293-TSPO cells treated with lorazepam (50 μ M) for 48 hours. * indicates statistical significance $p < 0.05$

3.2.3 The effect of TSPO overexpression on cell proliferation.

Although TSPO has been implicated in the regulation of proliferation, overexpression of TSPO in HEK293 cells had no effect on cell proliferation rates (Figure 15). Wild-type 293 cells, 293-TSPO and 293-C cells were counted each day for 4 days to determine cell proliferation rates.

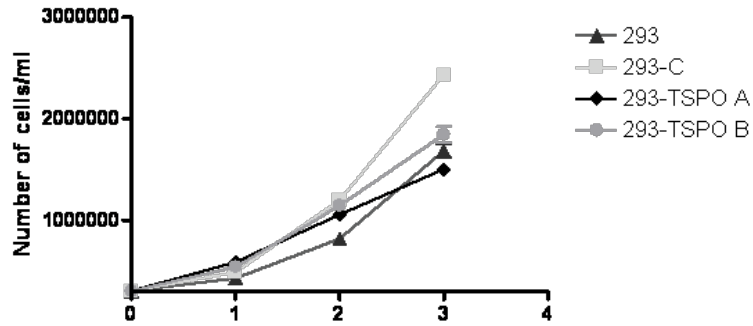


Figure 15. TSPO overexpression has no effect on HEK293 cell proliferation.

Direct cell counting of 293, 293-C, and 293-TSPO A/B cells over time.

3.2.4 TSPO knockdown in PPC-1 human prostate cancer cells.

Figure 16 shows the drastic decrease in TSPO expression (18kDa only) in PPC-1 human prostate cancer cells transfected with shRNA directed against TSPO. PPC-1 cells transfected with shTSPO will be referred to as shTSPO Y1 or Y2.

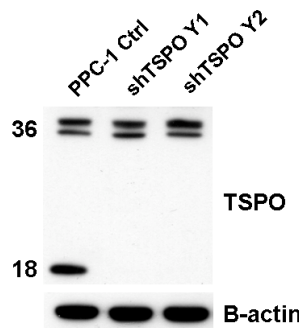


Figure 16. TSPO knockdown in PPC-1 cells.

PPC-1 Ctrl: empty vector control, shTSPO Y1/Y2: PPC-1 cells transfected with shRNA directed against TSPO. Immunoblots were reprobed for B-Actin to ensure equal loading.

3.2.5 The effect of TSPO knockdown on cell proliferation.

A radiolabelled thymidine incorporation assay was used to determine the effect of TSPO knockdown on cell proliferation. Figure 17 demonstrates that cell proliferation in the shTSPO Y2 clone was significantly affected by decreasing levels of TSPO; however the shTSPO Y1 clone was not.

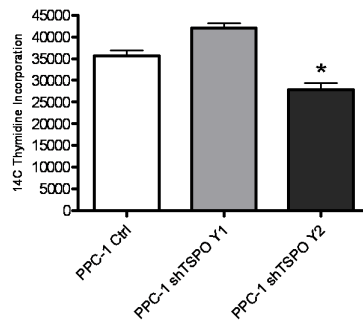


Figure 17. TSPO knockdown has differential effects on proliferation in PPC-1 shTSPO clones.

PPC-1 ctrl: empty vector control, PPC-1 shTSPO Y1/Y2: PPC-1 cells expression shTSPO. * indicates statistical significance $p < 0.05$

3.2.6 The effect of TSPO knockdown on cell susceptibility to lorazepam.

Decreasing levels of TSPO had no effect on susceptibility of the cells to TSPO antagonism by direct cell counting (Figure 18). PPC-1 empty vector controls and shTSPO Y1/Y2 clones were treated with 50 μ M lorazepam and cells were counted after 48 hours.

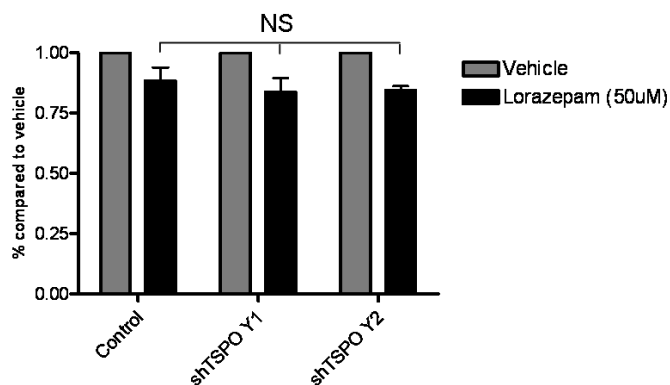


Figure 18. TSPO knockdown has no effect on PPC-1 cells susceptibility to lorazepam by direct cell counting. Control: PPC-1 empty vector control cells, shTSPO Y1/Y2: PPC-1 cells expressing shTSPO, NS: not significant.

Preliminary evidence suggested that lorazepam was exhibiting its anti-cancer properties by working through TSPO. Therefore, it was expected that knocking down TSPO levels would decrease PPC-1 cells susceptibility to lorazepam induced inhibition of cell growth. There appeared to be no significant effect of TSPO knockdown on susceptibility to lorazepam through direct cell counting (Figure 18). To examine cell survival, a colony formation assay was utilized. PPC-1 empty vector controls and shTSPO Y1/Y2 clones were plated at a low density and treated with vehicle (DMSO), 50 μ M, or 100 μ M lorazepam for 48 hours. Regular growth medium was added back and colonies grew for approximately 2 weeks, were stained, and then counted. Figure 19 shows a significant difference in susceptibility of control cells to lorazepam compared to cells expressing shTSPO. The bar graph represents the percent of colonies relative to the vehicle.

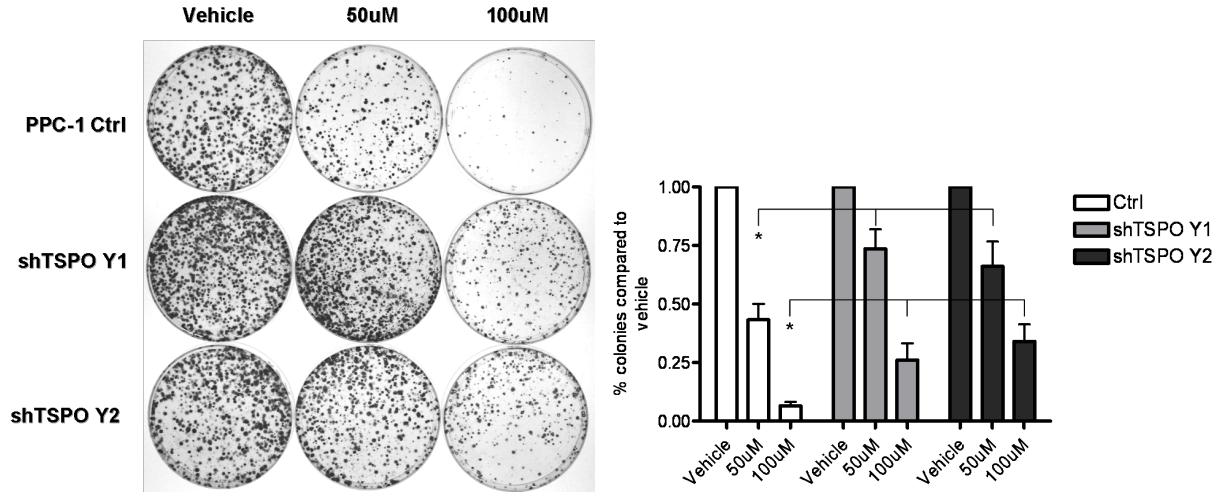


Figure 19. TSPO knockdown decreases PPC-1 cells susceptibility by colony formation assay.

Representative plates showing the colonies remaining following treatment with 50 or 100μM lorazepam. The bar graph represents the percent of colonies relative to the vehicle. * indicates statistical significance $p < 0.05$

3.2.7 The effect of TSPO knockdown on cell migration.

TSPO expression analysis of human prostate cancer tissues revealed that TSPO increases with progression, as prostate cancer metastases have the highest expression (Figure 4). This suggests that TSPO may be playing a role in metastatic-related events such as migration. A wound healing assay was used to determine a difference in the percent of control compared to shTSPO cells migrating into the wound. Figure 20 demonstrates that cell migration was reduced by decreasing levels of TSPO, as indicated by the significant decrease in percent wound closure.

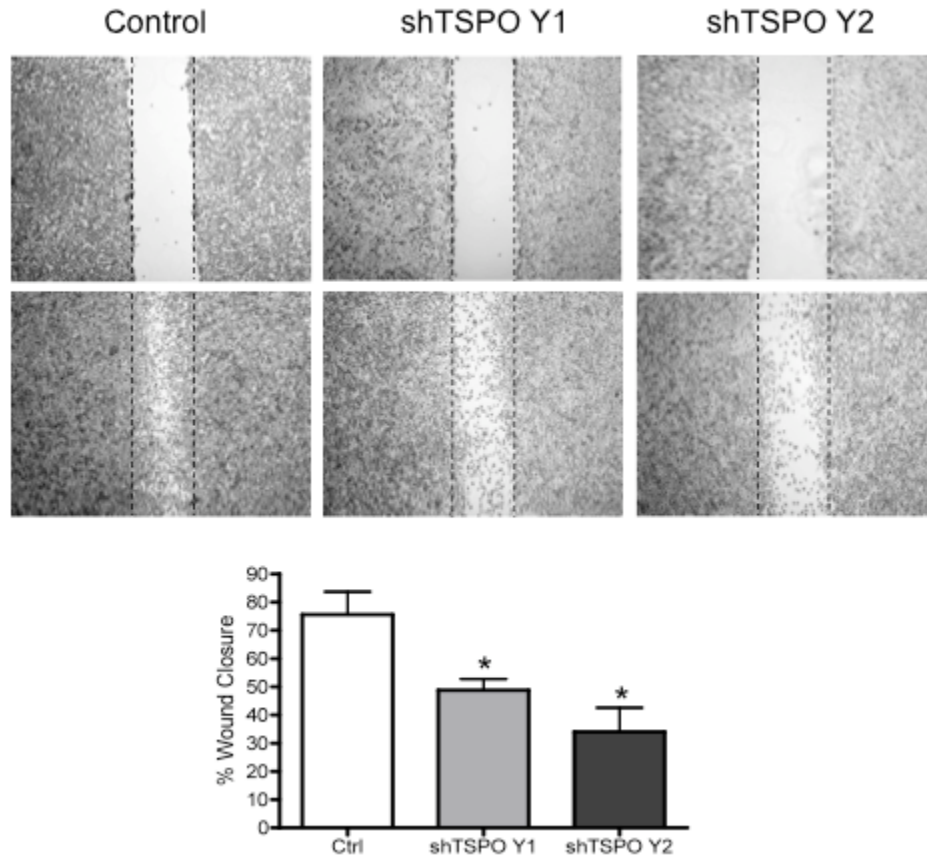


Figure 20. TSPO knockdown decreases cell migration in PPC-1 cells.

Representative images showing a significant decrease in cell migration into a wound upon TSPO knockdown. Control: PPC-1 empty vector cells, shTSPO Y1/Y2: PPC-1 cells expressing shTSPO. * indicates statistical significance $p < 0.05$

3.2.8 The effect of TSPO knockdown on cell growth in suspension.

Possessing the ability to grow in suspension is another characteristic of metastatic cancer cells. To determine if TSPO plays a role in this process, PPC-1 control and PPC-1 shTSPO cells were grown in soft agar. After approximately 3 weeks, colonies were counted in 4 different fields and the number of colonies per field was averaged. Knockdown of TSPO in PPC-1 cells resulted in a

significant decrease in the shTSPO Y2 clone but not the shTSPO Y1 clone, although a decreasing trend was observed (Figure 21).

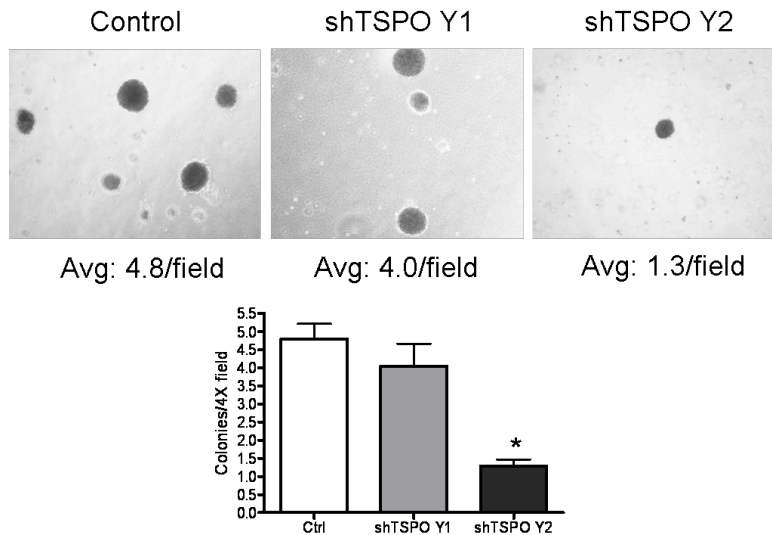


Figure 21. TSPO knockdown decreases PPC-1 cells ability to form colonies in suspension.

Soft agar colony formation assay of PPC-1 empty vector control cells compared to PPC-1 shTSPO Y1/Y2 clones. * indicates statistical significance $p < 0.05$

3.2.9 The effect of TSPO knockdown on cell invasion.

The ability to invade through the extracellular matrix is a requirement for metastatic cancer cells leaving the primary site. To determine if TSPO knockdown has an effect on this process, a Matrigel invasion assay was employed. Figure 22 demonstrates a decreasing trend of invasion in PPC-1 cells expressing shTSPO compared to empty vector control cells; however these data were not significant. There appears to be fewer shTSPO PPC-1 cells that invade through the control chamber as well, indicating that the role of TSPO may have a greater impact on migration rather than invasion.

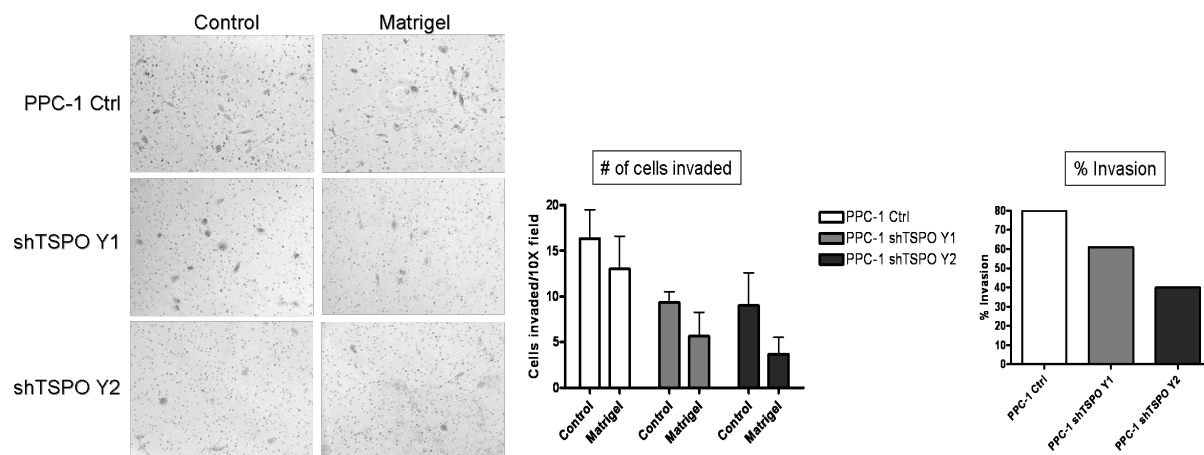


Figure 22. TSP0 knockdown decreases cell invasion in PPC-1 cells.

Matrigel invasion assay of PPC-1 empty vector control cells compared to PPC-1 shTSPO Y1/Y2 clones. PPC-1 Ctrl: PPC-1 empty vector cells, shTSPO Y1/Y2: PPC-1 cells expressing shTSPO. Control: inserts not containing matrigel, Matrigel: inserts containing matrigel.

3.3 CONCLUSIONS

The main purpose for the TSP0 overexpression study was to provide further evidence that lorazepam was exerting its anti-cancer effects through TSP0. Human embryonic kidney cells were utilized for these studies because they express relatively low endogenous levels of TSP0 compared to numerous prostate cancer cell lines (Figure 5). It was hypothesized that HEK293 cells overexpressing TSP0 would be more susceptible to lorazepam treatment. The data presented here support this hypothesis, as shown by the decrease in cell numbers (approximately 25%) following lorazepam treatment (Figure 14). Although an increase in sensitivity to lorazepam was observed, the overexpression of TSP0 alone did not alter the rate of cell proliferation, suggesting that modulation of cell proliferation is through TSP0 ligand binding.

Similar to the overexpression studies, TSPO knockdown was performed to determine if modulating TSPO expression affects susceptibility to lorazepam. Direct cell counting showed that decreasing TSPO levels had no effect on PPC-1 cells susceptibility to lorazepam (Figure 18). This may be due to the fact that only the monomeric form of TSPO (18kDa band) was efficiently knocked down; while the dimer (36kDa band) remained high, supporting that lorazepam may be acting through the dimeric form of TSPO. In contrast, colony formation assays revealed a decrease in susceptibility in PPC-1 cells expressing shTSPO compared to the empty vector controls (Figure 19), suggesting TSPO may play a role in cell survival but not cell growth.

TSPO expression analysis of human prostate cancer tissues revealed that TSPO increases with progression, as prostate cancer metastases have the highest expression (Figure 4). This suggests that TSPO may be playing a role in metastatic-related events such as migration, growth in suspension, and invasion. The studies presented here provide evidence for a role for TSPO in these processes as a decreasing trend in migration, growth in suspension, and invasion was observed.

4.0 THE ROLE OF TSPO MULTIMERS IN PROSTATE CANCER

4.1 INTRODUCTION

Studies over the past decade demonstrated that TSPO antibodies identify immunoreactive proteins of higher molecular weight than the expected 18-kDa in cell and tissue extracts. These molecular weights may correspond to TSPO multimers whose origin and formation are unknown. The first paper reporting the isolation of the 18-kDa TSPO protein also identified proteins of 32-36 and 50-54-kDa molecular size that were radiolabeled by PK14105, a TSPO specific ligand, in CHO hamster ovary mitochondrial cell extracts [32]. Follow-up reports on the presence of a 32-36-kDa protein showed that these TSPO polymers bind exclusively to TSPO drug ligands [32, 87-90]. The observation that the 18-kDa TSPO protein was organized in clusters of 2-7 molecules on the Leydig cell mitochondrial membrane suggested for the first time the presence of TSPO multimers [91]. The hormone-induced appearance of bigger TSPO clusters simultaneous with the appearance of a higher initiation of cholesterol transfer into mitochondria and steroidogenesis indicated that the formation of these clusters might be part of a functional process [92].

It is well documented that cancer cells have increased levels of free radicals compared to normal, noncancerous cells. A serendipitous connection was made when researchers observed that increased TSPO multimers corresponded to increased levels of intracellular reactive oxygen species (ROS) [46]. Additional studies found that treatment with reactive oxygen species

resulted in molecular mass complexes of TSPO ranging from 30-200kDa both *in vitro* and *in vivo*, suggesting a role for ROS in multimer formation [46].

Spectroscopic studies by Delavoie *et al.* strongly suggested that TSPO multimers are the result of di-tyrosine bonds that covalently link TSPO monomers through reactions mediated by reactive oxygen species [46]. The presence of TSPO trimers and tetramers suggested that there are at least two tyrosines per monomer involved in the polymer formation in a covalent manner. A di-tyrosine bond is an oxidative covalent cross-link between two tyrosines and is a product of normal posttranslational processes. Di-tyrosine crosslinking is identified as a marker for oxidative stress and has been detected in numerous pathologies. The studies presented in this chapter investigate the functional significance of TSPO multimers in advanced prostate cancer.

4.2 RESULTS

4.2.1 TSPO Multimers in TRAMP and Human Tissue

TSPO multimer expression was analyzed in lung, lymph node, and prostate tissue obtained from Transgenic Adenocarcinoma of Mouse Prostate (TRAMP) mice. Figure 23 A demonstrates a significant increase in TSPO expression in normal compared to matching cancerous tissue, and particularly an increase in the 36-kDa band, corresponding to the dimeric form of TSPO. Tissue from human primary prostate cancer was also examined and results showed no significant trend with increased multimers and disease aggressiveness (Figure 23 B).

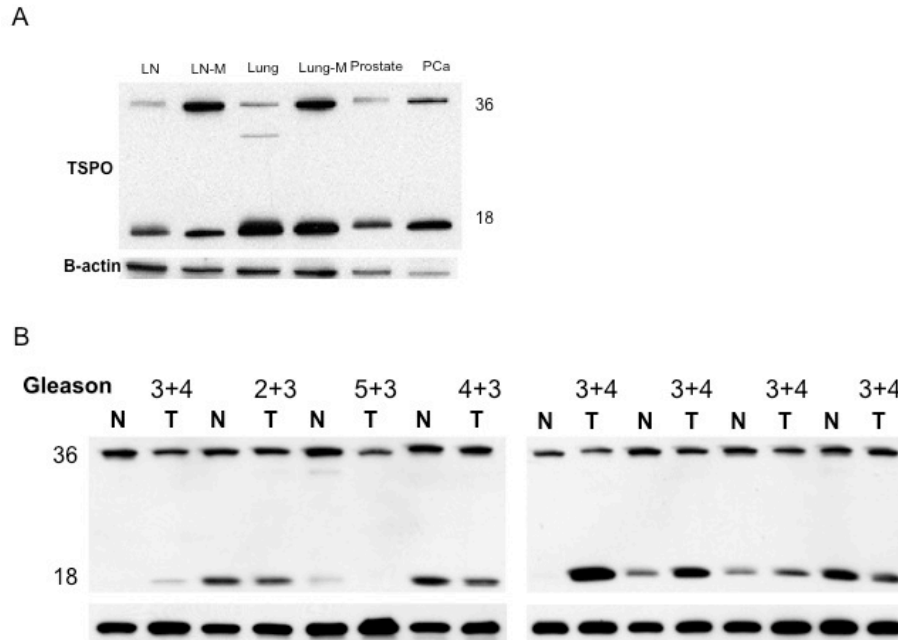


Figure 23. TSPO multimers in TRAMP and human tissues.

A. Increased TSPO multimer expression (36-kDa) in TRAMP lymph node metastases (LN-M), lung metastases (Lung-M), and primary prostate cancer (PCa) compared to corresponding nontumorigenic tissues. Number of mice screened included: 8 intact wildtype C57xFVB, intact TRAMP with primary tumor only, and intact TRAMP with mets (6 lung; 6 lymph node) B. TSPO multimer expression in human primary prostate cancer tissue (T) compared to normal tissue adjacent to the tumor (N). Gleason grade had no effect on the levels of TSPO multimers present.

4.2.2 Transient Knockdown of TSPO Multimers

TSPO multimer status of PPC-1 cells treated with siRNA directed against TSPO was examined at 0, 24, 48, 72, 96, 120, 144, 168, and 192 hours post transfection. After 48 hours the 18-kDa band was approximately 80% knocked down, while the 36-kDa band remained as high as the control (Figure 24). The 36-kDa band was briefly decreased at 72 hours, but recovered by 96 hours. Interestingly, the 18-kDa band remained knocked down until 144 hours and did not fully recover until 192 hours (Figure 24). A scrambled siRNA was used as a control.

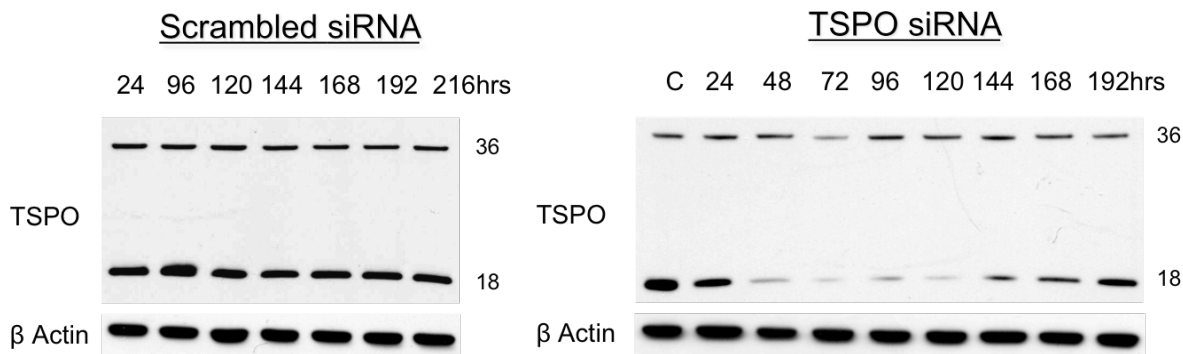


Figure 24. TSPO multimer status following transfection with TSPO siRNA.

Western blot analysis of TSPO expression in PPC-1 cells transfected with scrambled siRNA or siRNA directed against TSPO for 24-192 hours. C: control cells collected at time of transfection.

4.2. 8M Urea Does Not Break Di-Tyrosine Bonds

Previous studies have suggested that a solution of 8M Urea is sufficient to break di-tyrosine bonds. PPC-1 cells treated with 8M Urea had no significant change in TSPO multimer status (Figure 25).

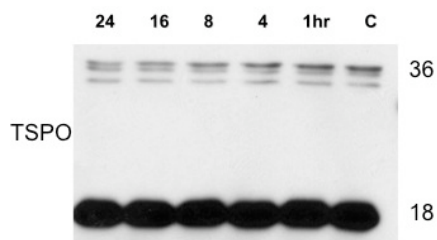


Figure 25. 8M Urea does not break TSPO multimer bonds.

Western blot analysis of PPC-1 cells treated with 8M Urea from 1-24 hours. C: untreated PPC-1 cells.

4.2.4 Hydrogen Peroxide Induces TSPO Multimer Formation

Hydrogen peroxide (H_2O_2) generates reactive oxygen species and was therefore used in these studies to determine the effect of increasing ROS on TSPO multimer formation. H_2O_2 treatment increased TSPO multimer formation (108-kDa band) in HEK293 cells overexpressing TSPO compared to HEK293 controls and HEK293 TSPO cells not treated with H_2O_2 (Figure 26).

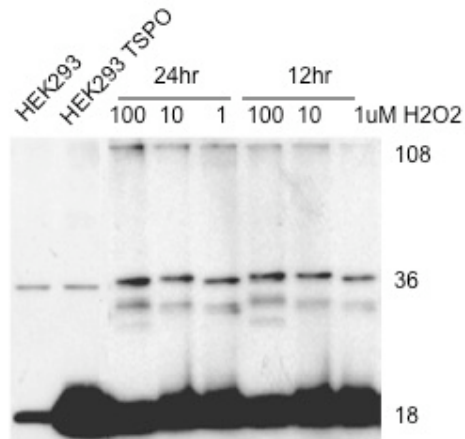


Figure 26. Hydrogen peroxide induces TSPO multimer formation in HEK293 cells.

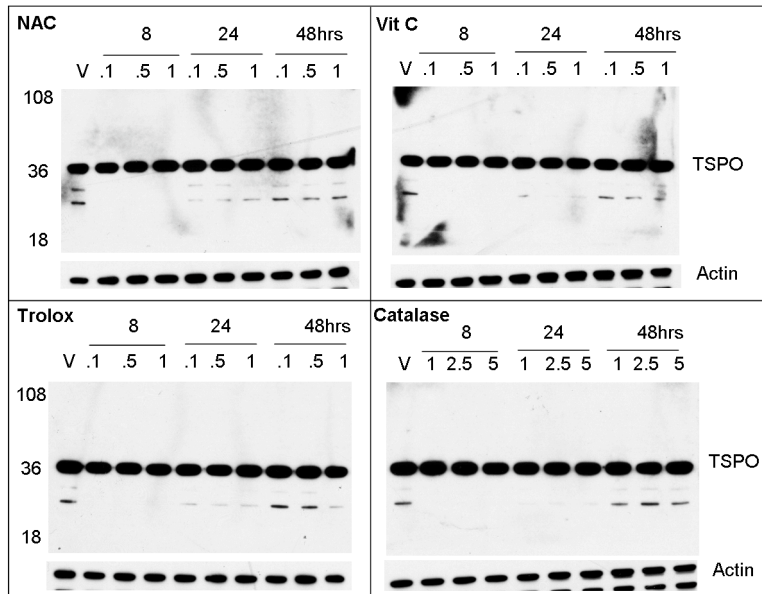
Western blot analysis of TSPO showing an increase TSPO multimer formation in HEK293 TSPO cells treated with H_2O_2 compared to HEK293 and untreated HEK293 TSPO cells. HEK293 TSPO: HEK293 cells overexpressing TSPO.

4.2.5 Reactive Oxygen Species Scavengers Increase TSPO Monomers

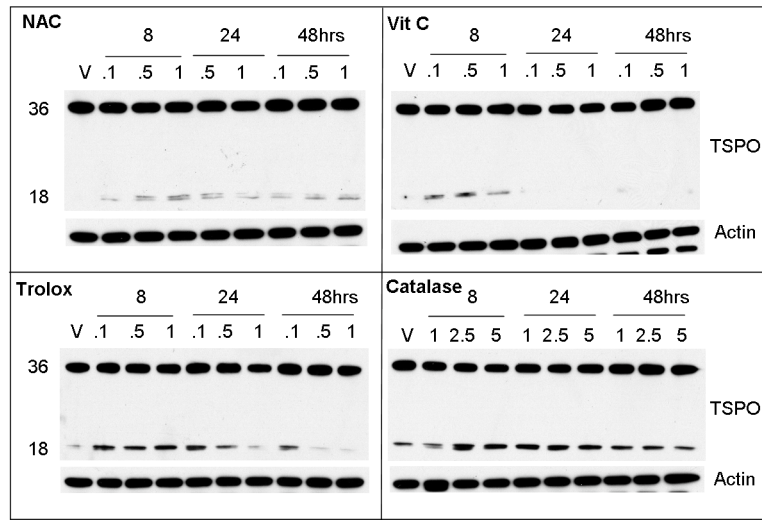
MLL cells lack the 18-kDa monomeric form of TSPO and were therefore used for these studies. Parental MLL and MLL cells overexpressing TSPO were treated with 4 different ROS scavengers at various time points. Different forms of ROS may be responsible for di-tyrosine bond formation; therefore we utilized four different ROS scavengers that targeted several of the intracellular sources of ROS. N-acetylcysteine dramatically increased the production of

glutathione, the most abundant ROS scavenger in many cells. Ascorbic acid and Trolox are water-soluble ROS scavengers, and catalase is an enzyme that functions to catalyze the decomposition of hydrogen peroxide to water and oxygen. In these studies we found that ROS scavengers had no effect on MLL cells but “stabilized” the 18-kDa monomer in MLL cells overexpressing TSPO (Figure 27).

MLL



MLL TSPO A



MLL TSPO B

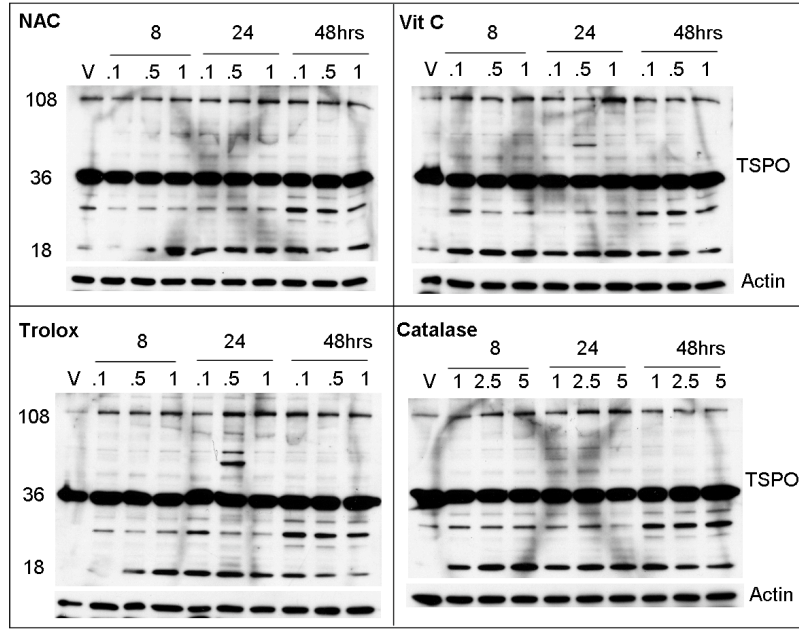


Figure 27. ROS scavengers increase TSPO monomers in MLL TSPO cells.

Western blot analysis of TSPO expression in MLL and MLL TSPO cells (MLL TSPO A or B) treated with ROS scavengers N-acetylcysteine (NAC), Vitamin C (Vit C), or Trolox at .1, .5, 1 μ M or Catalase at 1, 2.5, or 5 units/ml for 8, 24, or 48 hours.

4.2.6 Y34F Mutagenesis Does Not Abolish TSPO Multimer Formation

In an attempt to determine if di-tyrosine bonds were responsible for TSPO multimer formation, site-directed mutagenesis of a single tyrosine residue in TSPO was performed. There are 10 tyrosine residues in the TSPO protein (Figure 28), however we focused our attention on tyrosine 34 (Y34). Using the guidance of structural biologist Dr. Klein-Seetharaman, we identified Y34 as the one most likely to be involved in bond formation because 1) it is highly conserved throughout evolution and 2) it is the most accessible TSPO tyrosine residue based on TSPO

structure (the majority of the others are embedded in the mitochondrial membrane spanning regions of TSPO – see figure 28).

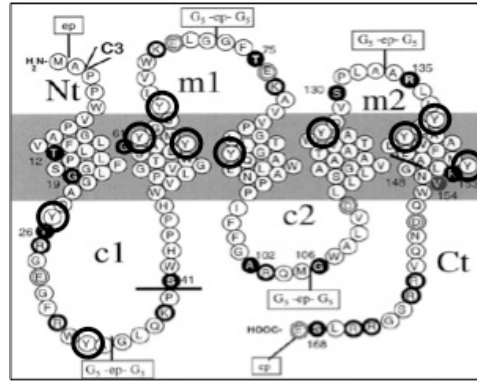


Figure 28. TSPO structure and location of tyrosines.

Black circles indicate a tyrosine residue. C1/C2: cytoplasmic loops, M1/M2: mitochondrial loops. (modified from Joseph-Liauzun *et al.* 1998)

A construct containing full length TSPO with a mutation of Y34 to phenylalanine (F34) was transiently transfected into HEK293, PPC-1, and MLL cells and screened 72 hours post-transfection. PPC-1 and HEK293 cells transfected with the SDM construct generated TSPO multimers at 108-kDa, corresponding to the TSPO 6-mer, suggesting that mutagenesis of this particular tyrosine in TSPO does not abolish multimer formation (Figure 29). MLL cells endogenously express the 6-mer and the data suggested no difference in multimer levels in these cells (Figure 29).

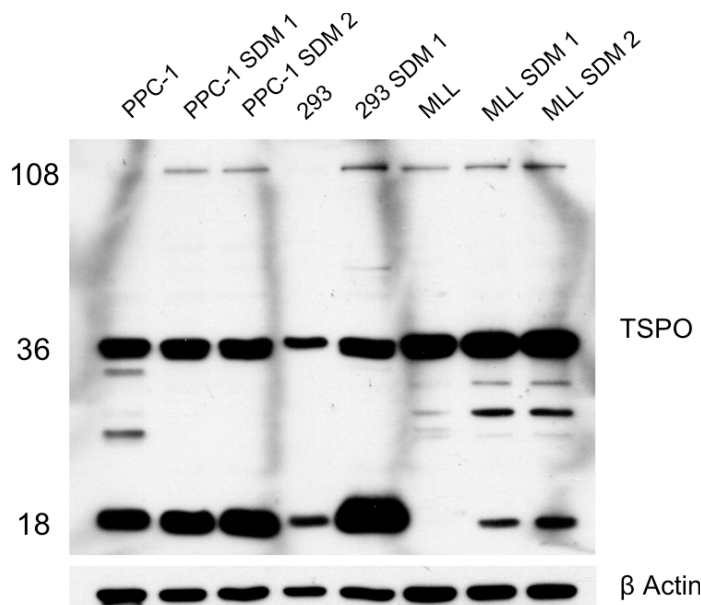


Figure 29. Site-directed mutagenesis of Y34 does not abolish TSP0 multimer formation.

Western blot analysis of PPC-1, HEK293, and MLL cells transfected with a TSP0 construct containing a mutation Y34 → F34 72 hours post-transfection. SDM 1/2: pooled samples of cells transfected with the SDM construct.

4.2.7 Glucose Oxidase Increases TSP0 Monomers in MLL SDM Cells

MLL cells overexpressing the TSP0 construct containing the Y34 → F34 mutation (MLL SDM) or MLL Neo (empty vector controls) were treated with the enzyme glucose oxidase at varying concentrations for 6 hours. Glucose oxidase was utilized because it is an enzyme that produces large amounts of hydrogen peroxide in the cell, thus increasing levels of ROS. Glucose oxidase treatment of MLL Neo cells resulted in a ~95% decrease in the 36-kDa band in all treatment conditions except at .01units/ml (Figure 30). Interestingly, in the MLL SDM cells glucose oxidase decreased the 36-kDa while increasing the 18-kDa band. Beta-actin was used as a

loading control but glucose oxidase treatment had an effect on this protein as well as TSPO. Therefore, GAPDH was run to ensure protein was present in those lanes (Figure 30).

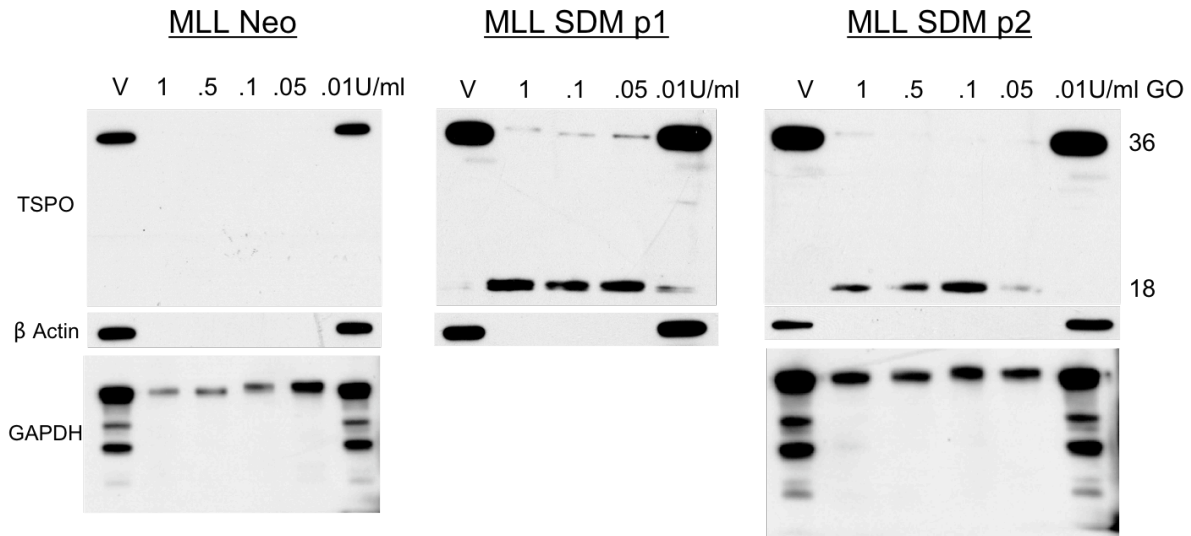


Figure 30. Glucose oxidase increases the 18-kDa TSPO monomer in MLL TSPO SDM cells.

Western blot analysis of TSPO multimer expression of MLL Neo (empty vector control) and MLL SDM (mutated tyrosine) cells treated with glucose oxidase at 1, .5, .1, .05, and .01 units/ml for 6 hours. β -Actin and GAPDH were used as loading controls.

4.3 CONCLUSIONS

The purpose of these studies was to determine whether di-tyrosine bonds are responsible for the higher molecular weight bands observed in our studies as well as to investigate the mechanism by which these bonds are formed. Immunoblot analysis of TSPO in TRAMP mouse tissues showed an increase in TSPO multimers (36-kDa bands) in both primary prostate cancer tissue and prostate cancer metastases compared to the matched normal tissues from the non-transgenic littermates. The monomeric 18-kDa band was ubiquitously expressed in all tissues, but the

increase in TSPO in cancer tissues occurs through elevated multimer (primarily 36-kDa) formation (Figure 23). These data suggest that TSPO multimers may be playing a role in advanced disease, as they appear to correlate with an increase in disease progression. Further evidence suggesting a functional importance for TSPO multimers was observed when TSPO was transiently down-regulated using siRNA directed against TSPO. These studies demonstrated that the 18-kDa band of TSPO can be significantly decreased with siRNA for up to 144 hours post transfection, while the 36-kDa band is marginally decreased at 72 hours (Figure 24). These data suggest that the dimeric form of TSPO is much more stable than the TSPO monomer.

Experiments attempting to break the bonds were unsuccessful, as 8M Urea has no significant effect on multimer formation (Figure 25). Conversely, hydrogen peroxide was shown to increase the 108-kDa band corresponding to a TSPO 6-mer (Figure 26). This supports previously published data suggesting that TSPO multimer formation is modulated by reactive oxygen species (ROS).

Formation of these stable multimers is believed to occur through di-tyrosine bonds formed by ROS [34]. Based on this hypothesis, ROS scavengers were used to determine if TSPO multimers can be decreased by inhibiting ROS production in the cells. Figure 27 demonstrates that ROS scavengers increase the 18-kDa band in MLL TSPO cells, suggesting that TSPO monomers can be “stabilized” by decreasing ROS levels. This was not observed in parental MLL cells, as these cells only express the dimeric form of TSPO.

In 2003, Delavoie *et al.* published data proposing that TSPO multimers were formed by a covalent bond between 2 tyrosine residues [46]. Using the expertise of a structural biologist, the tyrosine most likely based on structure to be involved in bond formation (Y34) was mutated to a phenylalanine. The hypothesis was that by creating an amino acid substitution of Y34 there

would be a decrease in TSPO multimers. Figure 29 demonstrates that overexpression of the mutagenic construct in PPC-1, 293, and MLL cells results in an increase in the 108-kDa band. These data provide evidence that tyrosine 34 by itself is not critical for TSPO bond formation. However, the Y34F substitution alters TSPO dimerization either indirectly or directly since we observed an increase in the higher molecular weight multimers. These data suggest that mutating this residue alters multimer formation possibly by changing the structure of TSPO to more readily allow covalent bonds to form. Alternatively, it is conceivable that tyrosine 34 forms a bond with another residue and a phenylalanine substitution more readily promotes formation of a covalent bond with this other residue.

Treatment of MLL cells overexpressing the mutated TSPO construct with glucose oxidase revealed an increase in the 18-kDa TSPO band and decrease in the 36-kDa band at relatively high concentrations (Figure 30). These data do not support the hypothesis that ROS increase multimers and warrant further studies. Hydrogen peroxide treated cell lysates showed a dose dependent increase in multimer formation but the glucose oxidase treatment increased the 18-kDa monomer. This may be due to the difference in experimental procedures, as cell lysates were treated with hydrogen peroxide while living cells were treated with glucose oxidase. The reverse experiments would need to be performed to determine if the same phenotype is observed.

The studies presented here provide further evidence that TSPO multimers are important for TSPO function; however, additional studies to identify pathways involved in the dimer formation and the tyrosines (or possibly other residues) that form the covalent bonds are required before a clear picture of the regulation of TSPO dimers and their impact on cell function can be made.

5.0 DISCUSSION

The main goal of these studies was to characterize TSPO expression in human prostate cancer and to determine its role as a potential therapeutic target for advanced disease. We have shown that TSPO expression is increased early in the neoplastic process, as prostatic intraepithelial neoplasia (PIN) has significantly increased levels of TSPO compared to normal prostate tissue and BPH (Figure 4). Moreover, we have demonstrated that TSPO expression increases with progression, as prostate cancer metastases have significantly more TSPO expression than all other tissues examined, including PIN and primary prostate cancer. Expression analysis *in vitro* suggests that TSPO is highly expressed in prostate cancer cell lines differing in their invasive abilities and androgen-sensitivity (Figure 5). Together our data support previous studies reporting that TSPO density is elevated in high-grade astrocytomas [74], glioblastomas [93], and highly aggressive breast cancer cell lines [57] compared to low-grade brain lesions and non-aggressive breast cancer cell lines. Similarly, Beinlich *et al.* reported that the TSPO ligand Ro5-4864 has the highest affinity binding capacity to TSPO in highly aggressive, estrogen receptor (ER) negative, progesterone receptor (PR) negative breast cancer cell lines BT-20 and MDA-MB-435-5 but binds with low capacity to TSPO in ER-positive, PR-positive nonaggressive MCF-7 and BT-474 breast cancer cell lines [94].

Several studies in the past decade have suggested that TSPO may play a role in carcinogenesis through its action as a modulator of cell proliferation and apoptosis. TSPO is highly expressed in steroidogenic cells, such as those of the testes and adrenals, of which TSPO ligands have been shown to regulate cell proliferation [95]. TSPO ligands have also been shown to affect proliferation and apoptosis in various tumors, such as astrocytomas, breast, esophageal, and colorectal [66, 74-76]. For our studies, we utilized one of the most common TSPO ligands, PK11195, as well as the benzodiazepine lorazepam, which has not previously been considered a TSPO antagonist. We demonstrated that both PK11195 and lorazepam have anti-proliferative and pro-apoptotic properties in prostate cancer cells *in vitro* (Figure 7 & 8).

Because lorazepam is a clinically approved drug that could easily be translated from preclinical studies to the prostate cancer patient population, we wanted to determine if lorazepam also exhibits anti-proliferative and pro-apoptotic actions *in vivo*. We observed a decrease in the length of time it took for the prostate cancer xenograft tumors to reach maximum size in the lorazepam treated mice compared to the vehicle group (Figure 11). Additionally, Ki67 expression, a protein marker for cell proliferation, and TUNEL, a marker of apoptosis, was decreased and increased, respectively, in the lorazepam treated group compared to mice given vehicle only (Figure 12). Together, these data further confirm that TSPO ligands modulate cell proliferation and apoptosis and provide continued evidence supporting the potential use of TSPO antagonists as anticancer drugs.

In all of our *in vitro* studies, PK11195 exhibited more potent anti-proliferative and pro-apoptotic effects than lorazepam (Figures 7 & 8). This is likely due to the difference in binding affinity, as PK11195 binds TSPO at nanomolar concentrations ($KD < 20nM$) [96]. Furthermore, it has been reported that lorazepam is significantly less potent than PK11195 at displacing

various ligands from TSPO binding sites [43]. However, lorazepam appears to have fewer off-target effects than PK11195 as the wildtype HEK293 cells with low TSPO expression had significant cell death with PK11195 but were minimally affected by lorazepam, while HEK293-TSPO overexpressing cells were susceptible to death by both compounds.

As demonstrated in Chapter 2, TSPO is highly expressed in human prostate cancer tissue and expression increases with progression. To understand the role of its up-regulation in advanced prostate cancer, we produced genetically modified human embryonic kidney cells, HEK293, and human prostate cancer cells, PPC-1, to overexpress and knockdown TSPO, respectively. HEK293 cells were chosen for the overexpression experiments because they express relatively low levels of TSPO compared to highly expressing prostate cancer cell lines, including PPC-1 cells. These modified cell lines were then used to evaluate the influence of TSPO density on the common features that drive invasive/aggressive phenotypes.

Transfection of a full-length TSPO construct into HEK293 cells resulted in a drastic increase in TSPO expression (Figure 13). Our hypothesis was that by increasing TSPO expression in low expressing cells, we would increase the cell's susceptibility to TSPO antagonists such as lorazepam. Figure 14 supports this hypothesis by demonstrating a 25% decrease in cell proliferation in HEK293 cells overexpressing TSPO compared to normal, non-transfected HEK293 cells treated with 50 μ M lorazepam. These data suggest that lorazepam is exhibiting its anti-proliferative effects through TSPO.

Transfection of shRNA directed against TSPO into PPC-1 cells resulted in a drastic decrease (~99%) in expression of the 18-kDa TSPO monomer but not the 36-kDa dimer (Figure 16). The inability to decrease the 36-kDa band is likely the result of a difference in stability of the monomer compared to the dimer. To determine the effects of TSPO knockdown on cell

proliferation, a thymidine incorporation assay was utilized. Using 2 different PPC-1 shTSPO clones, we observed an increase in proliferation rates in the Y1 clones and a significant decrease in the Y2 clones (Figure 17). This discrepancy is likely due to clonal variation and could be resolved using the pooled clones or retroviral transfection. Further experiments are necessary before any conclusions can be made regarding the effect of TSPO knockdown on cell proliferation.

Similar to the overexpression studies, we hypothesized that by decreasing TSPO the cells would be less susceptible to lorazepam treatment. Figure 18 shows that TSPO knockdown in PPC-1 has no significant effect on susceptibility to lorazepam as measured by cell proliferation. This may be due to the remaining 36-kDa TSPO dimer, which we believe is the functional unit of TSPO, therefore making the cells equally susceptible to the TSPO ligand. Interestingly, using a colony formation assay, we observed a significant decrease in susceptibility of PPC-1 TSPO cells to lorazepam compared to the empty vector control cells (Figure 19). At both 50 and 100 μ M concentrations of lorazepam PPC-1 shTSPO clones not only survived the treatment but they grew faster and had larger colonies compared to the empty vector control cells. Together these data suggest that decreasing TSPO does not affect modulation of cell proliferation rates by lorazepam but does affect the cells ability to survive the high concentration treatment.

In 2008, Rechichi *et al.* found that TSPO overexpression improved the motility rate and transmigration capability of C6 rat glioma cells, demonstrating that the increase of TSPO expression levels may contribute to the acquisition of an invasive/aggressive phenotype [83]. For our studies, we knocked down TSPO in order to determine if we could reduce the aggressive phenotype in characteristics of advanced disease such as migration, growth in suspension and invasion.

The ability of cells to migrate away from the primary tumor is a classic feature of advanced disease. Using a wound healing/scratch assay, we observed that decreasing TSPO significantly decreases the cells ability to migrate into the wound, as indicated by a decrease in percent closure of the wound (Figure 20). This data implicates a role for TSPO in cell migration, however future studies would be necessary to determine the molecular mechanisms by which this modulation in migration is occurring.

Similar to migration, the ability of a cancer cell to grow in suspension, such as when they travel through the bloodstream, is also a known characteristic of advanced cancer cells. In our studies, we found that by decreasing TSPO in PPC-1 cells, we were able to significantly decrease the number of colonies formed in suspension in soft agar (Figure 21). This is an indication of the cells ability to grow in suspension and not a differential effect in cell proliferation, as there was no difference in cell proliferation rates among the TSPO shRNA PPC-1 clones.

In order for a cancer cells to migrate through the extracellular matrix they need to possess the qualities necessary for degradation of the extracellular matrix and increasing motility factors. To determine if TSPO plays a role in cancer cell invasion, we utilized a Matrigel invasion assay and found a decreasing trend in invasion of those cells with decreased levels of TSPO. It is important to note that there was a slight, not statistically significant decrease in invasion through the Matrigel but there was a significant decrease in migration through the control inserts (Figure 22). This supports the wound healing/scratch assay results suggesting that knocking down TSPO affects cell migration but does not conclusively support a role for TSPO in cell invasion. Together these data suggest that TSPO expression may modulate regulation of motility factors such as the Rho family of GTPases, but does not affect cellular pathways leading to invasion,

such as those involved in the upregulation of matrix degrading factors such as matrix metalloproteinases.

Collectively, these data are the first direct evidence that TSPO density influences prostate cancer cell aggressiveness and is consistent with previous reports that correlate TSPO expression level and tumor malignancy grade [97-100].

To date, very little work has been devoted to understanding the significance of TSPO multimers, particularly in cancer. Our interest in this aspect of TSPO research began when we observed that not only was TSPO expression increased in transformed TRAMP tissues, but also the 36-kDa band was significantly increased, particularly in the metastatic tissue (Figure 23A). TSPO multimer expression analysis was also examined in human primary prostate cancer compared to normal tissue, however the increasing trend in TSPO multimers with disease progression was not observed (Figure 23B). The data was inconsistent which was not surprising, as human disease tissue is much more variable compared to tissue obtained from genetically identical transgenic mice.

In an attempt to transiently knockdown TSPO protein levels, we observed an interesting phenomenon. At 48 hours we were able to drastically decrease the 18-kDa TSPO band using siRNA directed against TSPO, however were not able to significantly knockdown the 36-kDa band (Figure 24). The fascinating part of this experiment was that the 18-kDa band was decreased for up to 144 hours post-transfection, while the 36-kDa band maintained normal expression patterns up to 192 hours, with the exception of 72 hours where it was decreased slightly (Figure 24). It is known that the half-life of the monomeric form of TSPO is approximately 3 days [101], however the unknown half-life of the dimer is likely to be much longer as indicated by the inability to decrease the dimer by decreasing the monomer. These

data support our hypothesis that the 36-kDa dimeric form of TSPO is more stable than the 18-kDa monomer, which may suggest that the dimeric form is the critical unit of TSPO.

In 2003, Delavoie *et al.* was the first to suggest that the detergent-resistant, multimeric forms of TSPO were the result of covalent crosslinking between tyrosine residues on two or more TSPO proteins [46]. Di-tyrosine bonds have been implicated in protein aggregation in other disease models such as alpha-synuclein polymers in Parkinson's disease and multiple systems atrophy [99]. Di-tyrosine bonds are believed to be a biomarker for oxidative stress, as reactive oxygen species are one of the driving forces behind the crosslinking [102].

Previous attempts have been made to break these extremely stable bonds through treatment with denaturing agents including 8M Urea and guanidinium chloride [99]. Figure 25 shows our unsuccessful attempt at breaking TSPO multimer bonds using 8M Urea. Extended time and heat did not break the covalent bond suggesting that the bonds are very stable. Because ROS have been implicated as the mechanism behind di-tyrosine bond formation, we determined the effect of hydrogen peroxide on TSPO multimer formation in HEK293 cells overexpressing the 18-kDa monomeric form of TSPO. We observed a dose-dependent increase in the TSPO 6-mer (corresponding to 108-kDa) following treatment with hydrogen peroxide (Figure 26). These studies support previous evidence suggesting that TSPO multimers are the result of di-tyrosine bond formation by ROS.

It is well documented that cancer cells have higher levels of ROS compared to normal cells. To further support the role of ROS in TSPO multimer formation, we utilized four different ROS scavengers to determine if decreasing intracellular levels of ROS could decrease TSPO multimers. MLL cells were used because they lack an endogenous 18-kDa TSPO but highly express the 36-kDa form. MLL cells overexpressing TSPO were also used to determine if

exogenous 18-kDa TSPO behaved differently in these cells. Using variable conditions, we made an interesting observation. Treatment of parental, MLL cells with ROS scavengers had no effect on TSPO multimer formation (Figure 27). Treatment of MLL-TSPO cells however, increased the amount of 18-kDa TSPO, suggesting that by decreasing ROS we were able to decrease multimer formation by “stabilizing” the 18-kDa monomer (Figure 27). It is important to note that although there was an increase in the 18-kDa band, there was not a corresponding decrease in the 36-kDa band, suggesting that the monomers that were being made by the foreign TSPO construct were being kept as monomers because of the lack of ROS which would have driven the immediate formation of the TSPO dimers.

If tyrosine residues are responsible for TSPO multimer formation, then mutation of a critical tyrosine residue should abolish bond formation. The TSPO protein has 10 tyrosine residues (Figure 28). Using the expertise of structural biologist Dr. Klein-Seetharaman, we identified the most likely tyrosine involved in bond formation based on TSPO structure. We concluded that there is one tyrosine (residue 34) that is highly conserved and readily accessible. A construct was designed that provided an amino acid substitution of the targeted tyrosine to a phenylalanine because it maintains the structure yet it lacks the hydroxyl group believed to be critical in bond formation. This mutated TSPO construct was transiently transfected in HEK293 (TSPO low expressing cells), PPC-1 (high expressing), and MLL (36-kDa expressing only). Figure 29 shows that despite the mutation in Y34, HEK293 and PPC-1 cells retained the ability to form the higher molecular weight multimers (108-kDa). There was no significant difference in multimer formation in MLL cells likely due to the fact that they normally express the 108-kDa band, unlike HEK293 and PPC-1 cells. These data suggest that Y34 by itself is not involved in di-tyrosine bond formation. Future studies could include site-directed mutagenesis of the other 9

tyrosines and/or combinational mutations, which would determine if more than one tyrosine is involved, or tagging of the mutagenic construct such that the movement of a monomer to a multimer could be observed, therefore distinguishing between endogenous and exogenous TSPO.

In our final multimer study, glucose oxidase, a hydrogen peroxide generating enzyme, was used to determine if TSPO multimers could be induced in MLL cells. After treatment of MLL cells overexpressing the mutated TSPO construct (MLL SDM TSPO) with glucose oxidase, we observed an interesting yet conflicting result. High concentrations of glucose oxidase abolished the 36-kDa band in both MLL empty vector control and MLL SDM TSPO cells. However, in the MLL SDM TSPO cells the 36-kDa band decreased as the 18-kDa band increased (Figure 30). These data do not support our ROS hypothesis, as we expected an increase in TSPO multimers with ROS treatment. It is important to note however, that the transfected construct contained the mutated TSPO protein; therefore this data may provide evidence that implicates tyrosine 34 in di-tyrosine bond formation. Treatment with high concentrations of glucose oxidase depleted the 36-kDa band, possibly due to protein degradation (see β -actin in Figure 30), however the mutation may have caused the newly produced TSPO to be maintained as a monomer. Much more work would need to be done before any correlations can be made between this tyrosine residue and TSPO multimer formation. Those experiments could include transfection of the non-mutated TSPO construct into MLL cells and glucose oxidase treatment, transfection of the mutated TSPO construct into HEK293 cells and glucose oxidase treatment, glucose oxidase treatment of PPC-1 cells to determine if the 36-kDa band is abolished.

Overall the multimer studies presented here are conflicting, neither convincingly supporting or refuting our hypothesis. Although trends seem to suggest a role for ROS in TSPO

bond formation, more work needs to be done to identify the pathways to fully comprehend this process. Understanding the importance of TSPO multimers in cancer is critical because it may be the key to targeting TSPO antagonists. If the dimer is the functional unit for TSPO, then finding a way to target the 36-kDa form may increase the anti-cancer effects of TSPO antagonists such as lorazepam.

Although benzodiazepines have been used clinically for over 50 years, their application as a form of cancer therapy is novel. We have shown that lorazepam, a benzodiazepine commonly prescribed to treat anxiety disorders, inhibits prostate cancer cell growth and survival. The studies presented here were designed to further elucidate the mechanism by which TSPO antagonists alter cancer cell proliferation and survival. In addition, this was the first study to examine the functional significance of TSPO multimers in cancer and identify the impact of the formation and inhibition of multimers. These studies were imperative in order to determine how modulation of TSPO expression and form alter cellular function while examining the potential application of lorazepam in cancer therapeutics. Antagonists for TSPO are already used in the clinic for other indications and demonstrate very minor side effects; therefore the translation of the preclinical results to the prostate cancer patient population could be readily achieved.

Based on the data presented here there is a significant amount of work left to be done to confirm the role of TSPO antagonism by benzodiazepines. Although the focus of our studies was on lorazepam, we are not limiting the possibility that other benzodiazepines may exhibit similar anti-cancer properties. An epidemiologic study looking at the use of benzodiazepines and prostate cancer progression would provide substantial evidence as to whether or not benzodiazepines are viable treatment options for advanced prostate cancer patients. The use of benzodiazepines could lead to a significant change in the management of prostate cancer by

providing a treatment option with minimal toxicity for use after failure of androgen-deprivation therapy and could ultimately prevent prostate cancer deaths.

BIBLIOGRAPHY

1. Saunders, J.B., de C.M. and O'Malley, C.D., *The illustrations from the works of Andreas Vesalius of Brussels*. Dover Publications Inc, New York., 1950.
2. Cole, F.J., *A history of comparative anatomy*. The Macmillan Press, London., 1949.
3. Lowsley, O.S., *The development of the human prostate gland with reference to the development of other structures at the neck of the urinary bladder*. Am J Anat, 1912. **13**: p. 299–349.
4. McNeal, J.E., *The prostate gland: morphology and pathobiology*. Monogr Urol 1983. **4**: p. 3–33.
5. Shannon, J.M. and G.R. Cunha, *Autoradiographic localization of androgen binding in the developing mouse prostate*. Prostate, 1983. **4**(4): p. 367-73.
6. Takeda, H., T. Mizuno, and I. Lasnitzki, *Autoradiographic studies of androgen-binding sites in the rat urogenital sinus and postnatal prostate*. Journal of Endocrinology, 1985. **104**(1): p. 87-92.
7. Takeda, H. and C. Chang, *Immunohistochemical and in-situ hybridization analysis of androgen receptor expression during the development of the mouse prostate gland*. Journal of Endocrinology, 1991. **129**(1): p. 83-9.
8. Lee, F., et al., *Use of transrectal ultrasound and prostate-specific antigen in diagnosis of prostatic intraepithelial neoplasia*. Urology, 1989. **34**(6 Suppl): p. 4-8.
9. Abate-Shen, C., Shen MM, *Molecular genetics of prostate cancer*. Genes Dev., 2000. **14**(19): p. 2410-34.
10. Hadley, H.L., *Physiology of the prostate*. Med Arts Sci., 1952. **6**(1): p. 22-23.
11. Jemal, A., et al., *Cancer statistics, 2008*. CA: a Cancer Journal for Clinicians, 2008. **58**(2): p. 71-96.

12. Williams, H. and I.J. Powell, *Epidemiology, pathology, and genetics of prostate cancer among African Americans compared with other ethnicities*. *Methods in Molecular Biology*, 2009. **472**: p. 439-53.
13. Endrizzi, B.J., et al., *Specific covalent immobilization of proteins through dityrosine cross-links*. *Langmuir*, 2006. **22**(26): p. 11305-10.
14. Witte, J.S., *Prostate cancer genomics: towards a new understanding*. *Nature Reviews Genetics*, 2009. **10**(2): p. 77-82.
15. Tomlins, S.A., et al., *Recurrent fusion of TMPRSS2 and ETS transcription factor genes in prostate cancer.[see comment]*. *Science*, 2005. **310**(5748): p. 644-8.
16. Tomlins, S.A., et al., *Distinct classes of chromosomal rearrangements create oncogenic ETS gene fusions in prostate cancer*. *Nature*, 2007. **448**(7153): p. 595-9.
17. Kumar-Sinha, C., S.A. Tomlins, and A.M. Chinnaiyan, *Recurrent gene fusions in prostate cancer*. *Nature Reviews Cancer*, 2008. **8**(7): p. 497-511.
18. Freedman, M., Christopher A. Haimanc, Nick Patterson Gavin J. McDonald, Arti Tandon, Alicja Waliszewskab, Kathryn Penneyb, Robert G. Steene, Kristin Ardlieb, Esther M. John, Ingrid Oakley-Girvan, Alice S. Whittemore, Kathleen A. Cooney, Sue A. Ingles, David Altshuler, Brian E. Hendersond, and David Reich, *Admixture mapping identifies 8q24 as a prostate cancer risk locus in African-American men*. *PNAS*, 2006. **103**(38): p. 14068-14073.
19. Mohamad, H., Apffelstaedt JP, *Counseling for male BRCA mutation carriers: a review*. *Breast*, 2008. **17**(5): p. 441-50.
20. Hayes, R.B., et al., *Dietary factors and risks for prostate cancer among blacks and whites in the United States*. *Cancer Epidemiology, Biomarkers & Prevention*, 1999. **8**(1): p. 25-34.
21. Giovannucci, E., et al., *A prospective study of dietary fat and risk of prostate cancer.[see comment]*. *Journal of the National Cancer Institute*, 1993. **85**(19): p. 1571-9.
22. Chan, J.M., P.H. Gann, and E.L. Giovannucci, *Role of diet in prostate cancer development and progression*. *Journal of Clinical Oncology*, 2005. **23**(32): p. 8152-60.
23. Bostwick, D.G., et al., *Human prostate cancer risk factors*. *Cancer*, 2004. **101**(10 Suppl): p. 2371-490.

24. Shavers, V.L., et al., *Race/ethnicity and the receipt of watchful waiting for the initial management of prostate cancer*. Journal of General Internal Medicine, 2004. **19**(2): p. 146-55.
25. Han, M., Gann, PH, Catalona, WJ, *Prostate-specific antigen and screening for prostate cancer*. Med Clin North Am, 2004. **88**(2): p. 245-65.
26. Fleshner, N. and A.R. Zlotta, *Prostate cancer prevention: past, present, and future*. Cancer, 2007. **110**(9): p. 1889-99.
27. *American Cancer Society*. 2007.
28. Feldman, B.J. and D. Feldman, *The development of androgen-independent prostate cancer*. Nature Reviews Cancer, 2001. **1**(1): p. 34-45.
29. Huggins, C., *Endocrine-induced regression of cancers*. Cancer Research, 1967. **27**(11): p. 1925-30.
30. Stoner, E., *The clinical development of a 5 alpha-reductase inhibitor, finasteride*. Journal of Steroid Biochemistry & Molecular Biology, 1990. **37**(3): p. 375-8.
31. Braestrup, C., R. Albrechtsen, and R.F. Squires, *High densities of benzodiazepine receptors in human cortical areas*. Nature, 1977. **269**(5630): p. 702-4.
32. Riond, J., et al., *Molecular cloning and chromosomal localization of a human peripheral-type benzodiazepine receptor*. European Journal of Biochemistry, 1991. **195**(2): p. 305-11.
33. Casalotti, S.O., et al., *Structure of the rat gene encoding the mitochondrial benzodiazepine receptor*. Gene, 1992. **121**(2): p. 377-82.
34. Lacapere, J.J. and V. Papadopoulos, *Peripheral-type benzodiazepine receptor: structure and function of a cholesterol-binding protein in steroid and bile acid biosynthesis*. Steroids, 2003. **68**(7-8): p. 569-85.
35. Papadopoulos, V., *Peripheral-type benzodiazepine/diazepam binding inhibitor receptor: biological role in steroidogenic cell function*. Endocrine Reviews, 1993. **14**(2): p. 222-40.
36. Verma, A. and S.H. Snyder, *Peripheral type benzodiazepine receptors*. Annual Review of Pharmacology & Toxicology, 1989. **29**: p. 307-22.
37. Galiegue, S., et al., *Cloning and characterization of PRAX-1. A new protein that specifically interacts with the peripheral benzodiazepine receptor*. Journal of Biological Chemistry, 1999. **274**(5): p. 2938-52.

38. Li, H., et al., *Identification, localization, and function in steroidogenesis of PAP7: a peripheral-type benzodiazepine receptor- and PKA (RIalpha)-associated protein*. *Molecular Endocrinology*, 2001. **15**(12): p. 2211-28.
39. McEnery, M.W., et al., *Isolation of the mitochondrial benzodiazepine receptor: association with the voltage-dependent anion channel and the adenine nucleotide carrier*. *Proceedings of the National Academy of Sciences of the United States of America*, 1992. **89**(8): p. 3170-4.
40. Decaudin, D., *Peripheral benzodiazepine receptor and its clinical targeting*. *Anti-Cancer Drugs*, 2004. **15**(8): p. 737-45.
41. Wang, J.K., J.I. Morgan, and S. Spector, *Benzodiazepines that bind at peripheral sites inhibit cell proliferation*. *Proceedings of the National Academy of Sciences of the United States of America*, 1984. **81**(3): p. 753-6.
42. Wang, J.K., T. Taniguchi, and S. Spector, *Structural requirements for the binding of benzodiazepines to their peripheral-type sites*. *Molecular Pharmacology*, 1984. **25**(3): p. 349-51.
43. Park, C.H., et al., *Characterization of peripheral benzodiazepine type sites in a cultured murine BV-2 microglial cell line*. *GLIA*, 1996. **16**(1): p. 65-70.
44. Joseph-Liauzun, E., et al., *Topological analysis of the peripheral benzodiazepine receptor in yeast mitochondrial membranes supports a five-transmembrane structure*. *Journal of Biological Chemistry*, 1998. **273**(4): p. 2146-52.
45. Anholt, R.R., et al., *The peripheral-type benzodiazepine receptor. Localization to the mitochondrial outer membrane*. *Journal of Biological Chemistry*, 1986. **261**(2): p. 576-83.
46. Delavoie, F., et al., *In vivo and in vitro peripheral-type benzodiazepine receptor polymerization: functional significance in drug ligand and cholesterol binding*. *Biochemistry*, 2003. **42**(15): p. 4506-19.
47. Brenner, C. and S. Grimm, *The permeability transition pore complex in cancer cell death*. *Oncogene*, 2006. **25**(34): p. 4744-56.
48. Marzo, I., et al., *Bax and adenine nucleotide translocator cooperate in the mitochondrial control of apoptosis*. *Science*, 1998. **281**(5385): p. 2027-31.

49. Kroemer, G., *The mitochondrial permeability transition pore complex as a pharmacological target. An introduction.* Current Medicinal Chemistry, 2003. **10**(16): p. 1469-72.
50. Hirsch, T., et al., *PK11195, a ligand of the mitochondrial benzodiazepine receptor, facilitates the induction of apoptosis and reverses Bcl-2-mediated cytoprotection.* Experimental Cell Research, 1998. **241**(2): p. 426-34.
51. Bono, F., et al., *Peripheral benzodiazepine receptor agonists exhibit potent antiapoptotic activities.* Biochemical & Biophysical Research Communications, 1999. **265**(2): p. 457-61.
52. Sutter, A.P., et al., *Peripheral benzodiazepine receptor ligands induce apoptosis and cell cycle arrest in human hepatocellular carcinoma cells and enhance chemosensitivity to paclitaxel, docetaxel, doxorubicin and the Bcl-2 inhibitor HA14-1.* Journal of Hepatology, 2004. **41**(5): p. 799-807.
53. Maaser, K., et al., *Cell cycle-related signaling pathways modulated by peripheral benzodiazepine receptor ligands in colorectal cancer cells.* Biochemical & Biophysical Research Communications, 2004. **324**(2): p. 878-86.
54. Sutter, A.P., et al., *Enhancement of peripheral benzodiazepine receptor ligand-induced apoptosis and cell cycle arrest of esophageal cancer cells by simultaneous inhibition of MAPK/ERK kinase.* Biochemical Pharmacology, 2004. **67**(9): p. 1701-10.
55. Li, J., J. Wang, and Y. Zeng, *Peripheral benzodiazepine receptor ligand, PK11195 induces mitochondria cytochrome c release and dissipation of mitochondria potential via induction of mitochondria permeability transition.* Eur J Pharmacol, 2007. **560**(2-3): p. 117-22.
56. Hager, M.H., K.R. Solomon, and M.R. Freeman, *The role of cholesterol in prostate cancer.* Curr Opin Clin Nutr Metab Care, 2006. **9**(4): p. 379-85.
57. Hardwick, M., et al., *Peripheral-type benzodiazepine receptor (PBR) in human breast cancer: correlation of breast cancer cell aggressive phenotype with PBR expression, nuclear localization, and PBR-mediated cell proliferation and nuclear transport of cholesterol.* Cancer Research, 1999. **59**(4): p. 831-42.
58. Sakai, M., et al., *Effects of peripheral-type benzodiazepine receptor ligands on Ehrlich tumor cell proliferation.* Eur J Pharmacol, 2006. **550**(1-3): p. 8-14.

59. Reszka, A.A., J. Halasy-Nagy, and G.A. Rodan, *Nitrogen-bisphosphonates block retinoblastoma phosphorylation and cell growth by inhibiting the cholesterol biosynthetic pathway in a keratinocyte model for esophageal irritation*. *Mol Pharmacol*, 2001. **59**(2): p. 193-202.
60. Carmel, I., et al., *Peripheral-type benzodiazepine receptors in the regulation of proliferation of MCF-7 human breast carcinoma cell line*. *Biochemical Pharmacology*, 1999. **58**(2): p. 273-8.
61. Batra, S., et al., *Characterization of peripheral benzodiazepine receptors in rat prostatic adenocarcinoma*. *Prostate*, 1994. **24**(5): p. 269-78.
62. Katz, Y., et al., *Increased density of peripheral benzodiazepine-binding sites in ovarian carcinomas as compared with benign ovarian tumours and normal ovaries*. *Clinical Science*, 1990. **78**(2): p. 155-8.
63. Batra, S., et al., *Peripheral benzodiazepine receptor in human endometrium and endometrial carcinoma*. *Anticancer Research*, 2000. **20**(1A): p. 463-6.
64. Beinlich, A., et al., *Relation of cell proliferation to expression of peripheral benzodiazepine receptors in human breast cancer cell lines*. *Biochemical Pharmacology*, 2000. **60**(3): p. 397-402.
65. Sutter, A.P., et al., *Specific ligands of the peripheral benzodiazepine receptor induce apoptosis and cell cycle arrest in human esophageal cancer cells*. *International Journal of Cancer*, 2002. **102**(4): p. 318-27.
66. Maaser, K., et al., *Specific ligands of the peripheral benzodiazepine receptor induce apoptosis and cell cycle arrest in human colorectal cancer cells*. *British Journal of Cancer*, 2001. **85**(11): p. 1771-80.
67. Decaudin, D., et al., *Peripheral benzodiazepine receptor ligands reverse apoptosis resistance of cancer cells in vitro and in vivo*. *Cancer Research*, 2002. **62**(5): p. 1388-93.
68. Han, Z., et al., *Expression of peripheral benzodiazepine receptor (PBR) in human tumors: relationship to breast, colorectal, and prostate tumor progression*. *Journal of Receptor & Signal Transduction Research*, 2003. **23**(2-3): p. 225-38.
69. Alenfall, J. and S. Batra, *Modulation of peripheral benzodiazepine receptor density by testosterone in Dunning G prostatic adenocarcinoma*. *Life Sci*, 1995. **56**(22): p. 1897-902.

70. Batra, S. and J. Alenfall, *Characterization of peripheral benzodiazepine receptors in rat prostatic adenocarcinoma*. *Prostate*, 1994. **24**(5): p. 269-78.
71. Katz, Y., A. Eitan, and M. Gavish, *Increase in peripheral benzodiazepine binding sites in colonic adenocarcinoma*. *Oncology*, 1990. **47**(2): p. 139-42.
72. Batra, S. and C.S. Iosif, *Peripheral benzodiazepine receptor in human endometrium and endometrial carcinoma*. *Anticancer Research*, 2000. **20**(1A): p. 463-6.
73. Brenner, C. and S. Grimm, *The permeability transition pore complex in cancer cell death.[erratum appears in Oncogene. 2006 Oct 26;25(50):6678]*. *Oncogene*, 2006. **25**(34): p. 4744-56.
74. Miettinen, H., et al., *Expression of peripheral-type benzodiazepine receptor and diazepam binding inhibitor in human astrocytomas: relationship to cell proliferation*. *Cancer Research*, 1995. **55**(12): p. 2691-5.
75. Papadopoulos, V., et al., *Drug-induced inhibition of the peripheral-type benzodiazepine receptor expression and cell proliferation in human breast cancer cells*. *Anticancer Research*, 2000. **20**(5A): p. 2835-47.
76. Sutter, A.P., et al., *Cell cycle arrest and apoptosis induction in hepatocellular carcinoma cells by HMG-CoA reductase inhibitors. Synergistic antiproliferative action with ligands of the peripheral benzodiazepine receptor*. *Journal of Hepatology*, 2005. **43**(5): p. 808-16.
77. Camins, A., et al., *A new aspect of the antiproliferative action of peripheral-type benzodiazepine receptor ligands*. *European Journal of Pharmacology*, 1995. **272**(2-3): p. 289-92.
78. Li, W., et al., *Peripheral-type benzodiazepine receptor overexpression and knockdown in human breast cancer cells indicate its prominent role in tumor cell proliferation*. *Biochem Pharmacol*, 2007. **73**(4): p. 491-503.
79. Alenfall, J. and S. Batra, *Modulation of peripheral benzodiazepine receptor density by testosterone in Dunning G prostatic adenocarcinoma*. *Life Sciences*, 1995. **56**(22): p. 1897-902.
80. Katz, Y., et al., *Identification and distribution of peripheral benzodiazepine binding sites in male rat genital tract*. *Biochemical Pharmacology*, 1990. **40**(4): p. 817-20.

81. Heinonen, O.P., et al., *Prostate cancer and supplementation with alpha-tocopherol and beta-carotene: incidence and mortality in a controlled trial.[see comment]*. Journal of the National Cancer Institute, 1998. **90**(6): p. 440-6.
82. Delavoie, F., et al., *In vivo and in vitro peripheral-type benzodiazepine receptor polymerization: functional significance in drug ligand and cholesterol binding*. Biochemistry, 2003. **42**(15): p. 4506-19.
83. Yeliseev, A.A. and S. Kaplan, *TspO of rhodobacter sphaeroides. A structural and functional model for the mammalian peripheral benzodiazepine receptor*. Journal of Biological Chemistry, 2000. **275**(8): p. 5657-67.
84. Calvo, D.J. and J.H. Medina, *Regulation of peripheral-type benzodiazepine receptors following repeated benzodiazepine administration*. Functional Neurology, 1992. **7**(3): p. 227-30.
85. Miller, L.G., et al., *Chronic benzodiazepine administration. I. Tolerance is associated with benzodiazepine receptor downregulation and decreased gamma-aminobutyric acidA receptor function*. Journal of Pharmacology & Experimental Therapeutics, 1988. **246**(1): p. 170-6.
86. Rechichi, M., et al., *TSPO over-expression increases motility, transmigration and proliferation properties of C6 rat glioma cells*. Biochimica et Biophysica Acta, 2008. **1782**(2): p. 118-25.
87. Snyder, S.H., A. Verma, and R.R. Trifiletti, *The peripheral-type benzodiazepine receptor: a protein of mitochondrial outer membranes utilizing porphyrins as endogenous ligands*. FASEB Journal, 1987. **1**(4): p. 282-8.
88. Lueddens, H.W., et al., *AHN 086: an irreversible ligand of "peripheral" benzodiazepine receptors*. Molecular Pharmacology, 1986. **29**(6): p. 540-5.
89. McCabe, R.T., et al., *[3H]AHN 086 acylates peripheral benzodiazepine receptors in the rat pineal gland*. FEBS Letters, 1989. **244**(2): p. 263-7.
90. Paul, S.M., E.S. Kempner, and P. Skolnick, *In situ molecular weight determination of brain and peripheral benzodiazepine binding sites*. European Journal of Pharmacology, 1981. **76**(4): p. 465-6.
91. Papadopoulos, V., et al., *Topography of the Leydig cell mitochondrial peripheral-type benzodiazepine receptor*. Molecular & Cellular Endocrinology, 1994. **104**(1): p. R5-9.

92. Boujrad, N., B. Vidic, and V. Papadopoulos, *Acute action of choriogonadotropin on Leydig tumor cells: changes in the topography of the mitochondrial peripheral-type benzodiazepine receptor*. *Endocrinology*, 1996. **137**(12): p. 5727-30.
93. Cornu, P., et al., *Increase in omega 3 (peripheral-type benzodiazepine) binding site densities in different types of human brain tumours. A quantitative autoradiography study*. *Acta Neurochirurgica*, 1992. **119**(1-4): p. 146-52.
94. Beinlich, A., et al., *Specific binding of benzodiazepines to human breast cancer cell lines*. *Life Sciences*, 1999. **65**(20): p. 2099-108.
95. Garnier, M., et al., *In vitro reconstitution of a functional peripheral-type benzodiazepine receptor from mouse Leydig tumor cells*. *Molecular Pharmacology*, 1994. **45**(2): p. 201-11.
96. Le Fur, G., et al., *Differentiation between two ligands for peripheral benzodiazepine binding sites, [3H]RO5-4864 and [3H]PK 11195, by thermodynamic studies*. *Life Sciences*, 1983. **33**(5): p. 449-57.
97. Vlodaysky, E., et al., *Immunohistochemical expression of peripheral benzodiazepine receptors in human astrocytomas and its correlation with grade of malignancy, proliferation, apoptosis and survival*. *Journal of Neuro-Oncology*, 2007. **81**(1): p. 1-7.
98. Veenman, L., et al., *Peripheral-type benzodiazepine receptor density and in vitro tumorigenicity of glioma cell lines*. *Biochemical Pharmacology*, 2004. **68**(4): p. 689-98.
99. Miettinen, H., et al., *Expression of peripheral-type benzodiazepine receptor and diazepam binding inhibitor in human astrocytomas: relationship to cell proliferation*. *Cancer Research*, 1995. **55**(12): p. 2691-5.
100. Miyazawa, N., et al., *Assessment of the peripheral benzodiazepine receptors in human gliomas by two methods*. *Journal of Neuro-Oncology*, 1998. **38**(1): p. 19-26.
101. Gavish, M., et al., *Enigma of the peripheral benzodiazepine receptor*. *Pharmacological Reviews*, 1999. **51**(4): p. 629-50.
102. Heinecke, J.W. and J.W. Heinecke, *Oxidized amino acids: culprits in human atherosclerosis and indicators of oxidative stress*. *Free Radical Biology & Medicine*, 2002. **32**(11): p. 1090-101.